Climate
of the Past

Discussions

EGU

Open Access

How dry was the Younger Dryas? Evidence from a coupled δ^2H-δ^{18}O biomarker paleohygrometer, applied to the Lake Gemündener Maar sediments, Western Eifel, Germany

Johannes Hepp[a,b,#,1], Lorenz Wüthrich[c], Tobias Bromm[b], Marcel Bliedtner[c,2], Imke Kathrin

5   Schäfer[c], Bruno Glaser[b], Kazimierz Rozanski[d], Frank Sirocko[e], Roland Zech[c,2], Michael

Zech[b,f,3]

[a]*Chair of Geomorphology and BayCEER, University of Bayreuth, Universitätsstrasse 30, D-95440 Bayreuth, Germany*

[b]*Institute of Agronomy and Nutritional Sciences, Soil Biogeochemistry, Martin-Luther-*

10   *University Halle-Wittenberg, Von-Seckendorff-Platz 3, D-06120 Halle, Germany*

[c]*Institute of Geography and Oeschger Center for Climate Change Research, University of Bern, Hallerstrasse 12, CH-3012 Bern, Switzerland*

[d]*Faculty of Physics and Applied Computer Science, AGH University of Science and Technology, Al. Mickiewicza 30, 30-059 Kraków, Poland*

15   [e]*Institute of Geosciences, Group of Climate and Sediments, Johannes Gutenberg University of Mainz, J.-J.-Becher-Weg 21, D-55128 Mainz, Germany*

[f]*Institute of Geography, Chair of Landscape- and Geoecology, Dresden University of Technology, Helmholtzstrasse 10, D-01062 Dresden, Germany*

20   [#] *corresponding author: johannes-hepp@gmx.de*

[1]Present Address: *Chair of Geomorphology and BayCEER, University of Bayreuth, Universitätsstrasse 30, D-95440 Bayreuth, Germany*
[2]Present Address: *Institute of Geography, Chair of Physical Geography, Friedrich-Schiller University of Jena, Löbdergraben 32, D-07743 Jena, Germany*
[3]Present Address: *Institute of Geography, Chair of Landscape- and Geoecology, Dresden University of Technology, Helmholtzstrasse 10, D-01062 Dresden, Germany*

Abstract

The Late Glacial to Early Holocene transition phase and particularly the Younger Dryas period, i.e. the major last cold spell in Central Europe during the Late Glacial, are considered crucial for understanding rapid natural climate change in the past. The sediments from Maar lakes in the Eifel, Germany, have turned out to be valuable archives for recording such paleoenvironmental changes.

For this study, we investigated a Late Glacial to Early Holocene sediment core that was retrieved from Lake Gemündener Maar in the Western Eifel, Germany. We analysed the hydrogen (δ^2H) and oxygen (δ^{18}O) stable isotope composition of leaf wax-derived lipid biomarkers (*n*-alkanes C_{27} and C_{29}) and hemicellulose-derived sugar biomarkers (arabinose), respectively. Both δ^2H and δ^{18}O are suggested to reflect mainly leaf water of vegetation growing in the catchment of the Gemündener Maar. This enables the coupling of the results via a δ^2H-δ^{18}O biomarker paleohygrometer approach and allows calculating past relative air humidity values, which is the major advantage of the applied approach. Fundamental was the finding that the isotopic enrichment of leaf water due to evapotranspiration depends mainly on relative humidity. We hence use the coupled δ^2H-δ^{18}O biomarker approach to reconstruct the deuterium-excess of leaf water and in turn relative air humidity values corresponding to the vegetation period and daytime (RH_{dv}).

Most importantly, the results of the coupled δ^2H-δ^{18}O biomarker paleohygrometer approach (i) support a two-phasing of the Younger Dryas, i.e. a relative wet phase (on Allerød level) followed by a drier Younger Dryas ending, (ii) do not corroborate overall drier climatic conditions characterising the Younger Dryas or a two-phasing with regard to a first dry and cold Younger Dryas phase followed by a warmer period along with increasing precipitation amounts, and (iii) suggest that the amplitude of RH_{dv} changes during the Early Holocene was more pronounced compared to the Younger Dryas. One possible driver for the unexpected Lake Gemündener Maar RH_{dv} variations could be the solar activity.

Climate
of the Past

Discussions

1 Introduction

In order to evaluate the relevance of man-made climate change in the future, it is of great importance to study and understand large and rapid climate fluctuations in the past. Many studies have focused on the Late Glacial to Early Holocene transition phase, a period with

5   various expressions in temperature, atmospheric circulation and hydrology worldwide (Alley, 2000; Brauer et al., 2008; Denton et al., 2010; Partin et al., 2015; Wagner et al., 1999). Particularly the Younger Dryas period, i.e. the major last cold spell in Central Europe during the Late Glacial just before the onset of the Holocene warm period (Denton et al., 2010; Heiri et al., 2014; Isarin and Bohncke, 1999), has long been considered crucial for understanding

10   rapid natural climate change in the past (Alley, 2000). The sediments from maar lakes in the Eifel, Germany, have turned out to be valuable archives for paleoenvironmental reconstructions providing high resolution palynological, sedimentological and geochemical records for climate, vegetation and landscape history (Brauer et al., 2008; Brunck et al., 2015; Litt et al., 2003; Litt and Stebich, 1999; Sirocko et al., 2013; Zolitschka, 1998).

15   Lacustrine sedimentary lipid biomarkers, originating either from leaf waxes of higher terrestrial plants (Eglinton and Hamilton, 1967) or from aquatic organisms (Volkman et al., 1998), and especially their hydrogen isotope composition ($\delta^2H_{n\text{-alkane}}$), are widely accepted as paleoclimate proxies (Huang et al., 2004; Mügler et al., 2008; Sachse et al., 2004; Sauer et al., 2001) demonstrating that the hydrogen isotope composition of the leaf waxes is well correlated

20   with hydrogen isotope composition of precipitation (δ^2H_{prec}) (Hou et al., 2008; Rao et al., 2009). This confirms the great potential to establish records of the stable isotope composition of past precipitation (Sachse et al., 2012), similar to the well-known ice-core records from Greenland and from speleothems (Alley, 2000; Luetscher et al., 2015; Rasmussen et al., 2014), which among others provide information about changes of surface air temperature in the past

25   (Dansgaard, 1964; Rozanski et al., 1993). However, the alteration of precipitation stable isotope signal either through leaf or lake water enrichment can challenge a direct reconstruction of δ^2H_{prec} based on $\delta^2H_{n\text{-alkane}}$ alone (Kahmen et al., 2013a; Mügler et al., 2008; Sachse et al., 2012). Apart from $\delta^2H_{n\text{-alkane}}$, the oxygen isotope composition of hemicellulose/polysaccharide-derived sugars ($\delta^{18}O_{sugar}$) was established as a tool in paleoclimate research during the last years

30   (Zech et al., 2011, 2013a, 2014a). Analogous to $\delta^2H_{n\text{-alkane}}$, $\delta^{18}O_{sugar}$ is affected by the isotope composition of source water, which is closely related to the local precipitation ($\delta^{18}O_{prec}$), as well as by evapotranspirative ^{18}O enrichment (Tuthorn et al., 2014; Zech et al., 2013b, 2014b). However, the overall challenge of disentangling between the source water signal and changes caused by evapotranspiration can be potentially resolved by using a coupled δ^2H-$\delta^{18}O$ approach

(Henderson et al., 2010; Hepp et al., 2015, 2017; Tuthorn et al., 2015; Voelker et al., 2014, 2015; Zech et al., 2013a). While Voelker et al. (2014) presented a framework for using δ^2H and $\delta^{18}O$ of tree-ring cellulose in order to infer relative air humidity, Tuthorn et al. (2015) validated a coupled δ^2H-$\delta^{18}O$ approach using leaf wax-derived *n*-alkanes and hemicellulose-derived sugars, showing the potential to reconstruct mean relative air humidity changes along an Argentinian topsoil transect. Both approaches were successfully applied to loess-paleosol sequences (Hepp et al., 2017; Zech et al., 2013a) and sub-fossil wood (Voelker et al., 2015), whereas the δ^2H-$\delta^{18}O$ coupling using terrestrial biomarkers in lacustrine archives is still missing. Indeed, already Sternberg (1988) suggested the coupling of aquatic δ^2H of lipids and $\delta^{18}O$ cellulose in order to tangle lake water isotope composition more robustly, due to challenges of using δ^2H values of nitro-cellulose derived from lake sediments. Hence, coupled δ^2H-$\delta^{18}O$ biomarker approaches applied to lacustrine archives were used to decipher between lake water evaporation history and changes in the isotope composition of the lake water input (Henderson et al., 2010; Hepp et al., 2015), based on a combination of δ^2H of palmitic acid and $\delta^{18}O$ of carbonate as well as $\delta^2H_{n\text{-alkane}}$ and $\delta^{18}O_{sugar}$ records. Deriving quantitative relative humidity values is challenging without additional hydrological input parameters, due to past lake mass balance changes (e.g. Wolfe et al., 2001). However, quantitative paleoclimate changes from biomarker-isotope proxy data, like a relative humidity record, may be useful to assess atmospheric circulation pattern changes in the past (Voelker et al., 2015), which was so far challenging due to a lack of applicable quantitative model approaches (Feng et al., 2007; Rach et al., 2014). Terrestrial *n*-alkane and sugar biomarker-based isotope records from Lake Gemündener Maar sediments, which are coupled in a δ^2H-$\delta^{18}O$ paleohygrometer approach, have the potential to fill this gap by deriving a more robust relative air humidity record for Central Europe for the Late Glacial and Early Holocene transition.

This study was conducted based on the following objectives: (i) source identification of the sedimentary organic matter and the investigated *n*-alkanes and sugars (aquatic vs. terrestrial), (ii) reconstructing leaf water isotope composition based on compound-specific δ^2H and $\delta^{18}O$ values of the *n*-alkane and sugar biomarkers, (iii) reconstructing relative air humidity via the coupled $\delta^2H_{n\text{-alkane}}$-$\delta^{18}O_{sugar}$ paleohygrometer approach and (iv) inferring new implications for middle European paleoclimate history from the established Lake Gemündener Maar relative air humidity record for the Late Glacial and Early Holocene transition. Overall, the potentials and limitations of the coupled $\delta^2H_{n\text{-alkane}}$-$\delta^{18}O_{sugar}$ paleohygrometer approach applied to lacustrine archive will be discussed.

Climate
of the Past

Discussions

2 Material & Methods

2.1 Lake Gemündener Maar and sampling

Lake Gemündener Maar is located in the Eifel volcanic fields in western Germany at an altitude of 407 m a.s.l (50°10'39.853"N, 6°50'12.912"E; Fig. 1A and B; Sirocko et al., 2013).

5   The Maar was formed during a phreatomagmatic explosion within the local Devonian siltstone (greywacke) around 20-25 ka BP (Büchel, 1993). The lake is 39 m deep at maximum and has a diameter of roughly 300 m. Due to its formation conditions the lake is almost circular with a lake surface area of 75,000 m^2 and is surrounded by a small catchment (Fig. 1B), with an area of 430,000 m^2 (Scharf and Menn, 1992). The lake is fed by precipitation and groundwater (no

10   surface inflow present). The catchment area is furthermore steep and densely vegetated with broad-leaved trees (Fig. 1C). The investigated samples were taken from the 8 m Gemündener Maar core (GM1), which was taken at approximately 20 m water depth near the center of the maar (Fig. 1B) with a Livingston piston corer (UWITEC, Mondsee, Austria). The core is part of the Eifel Laminated Sediment Archive Project of the Institute for Geoscience at Johannes

15   Gutenberg University Mainz (Sirocko et al., 2013, 2016).

(Fig. 1)

2.2 Bulk analysis and age control

Total carbon (TC), total organic nitrogen (TON), bulk carbon isotope composition

20   ($\delta^{13}C_{TC}$) and nitrogen isotope composition ($\delta^{15}N$) were determined at the Institute of Agronomy and Nutritional Sciences, Soil Biogeochemistry, Martin-Luther-University Halle-Wittenberg, using an EuroVector EA 3000 elemental analyzer (Hekatech, Wegberg, Germany) coupled via a Conflo III Interface to a Delta V Advantage isotope ratio mass spectrometer (IRMS; both from Thermo Fisher Scientific, Bremen, Germany). Additionally, total organic carbon (TOC)

25   and bulk $\delta^{13}C$ of the total organic carbon ($\delta^{13}C_{TOC}$) were assessed after removal of carbonate with 32% HCl fumigation followed by a neutralization step with moist NaOH, both for 24 h under 60°C and vacuum conditions. This allows calculating carbon to nitrogen ratio based on total organic contents (TOC/TON). Laboratory standards from the International Atomic Energy Agency (IAEA) as well as from United States Geological Survey (USGS) with known total

30   carbon, nitrogen, ^{13}C and ^{15}N contents (IAEA N2, IAEA CH6, IAEA NO3, IAEA CH7, IAEA 305A, USGS 41) were used for calibration. The ^{13}C and ^{15}N contents are expressed in the common δ-notation as relative to an international standard ($\delta^{13}C$: Vienna Pee Dee Belemnite, VPDB; $\delta^{15}N$: atmospheric N$_2$, Air). It should be noted that TON and ^{15}N contents are only reported for measurements prior to carbonate removal. This is based on Walthert et al. (2010)

Climate
of the Past

Discussions

and Harris et al. (2001), who reported lower N contents and slightly more positive $\delta^{15}N$ after HCl fumigation, respectively. Bulk analyses were carried out on 112 samples, covering a section of 606 cm to 727 cm depth of the Lake Gemündener Maar GM1 core.

The investigated sediments are partially laminated and the Laacher See Tephra (673 to
5   680 cm core depth; Fig. 2A) is clearly visible. The latter can be used as chronological marker due to the varve counted age of 12,880 a BP in the adjacent Meerfelder Maar (Fig. 2C; Brauer et al., 1999). The second tie point to establish a chronology for the Lake Gemündener Maar core is a radiocarbon-dated piece of charcoal in 727 cm core depth, which dated to 13,800 ± 110 cal a BP (Fig. 2C). This age is derived from a ^{14}C age of 11,950 ± 65 a BP as part of the
10   supplement material of Sirocko et al. (2013), calibrated using CalPal-software (Weninger and Jöris, 2008) calculated with the IntCal13 calibration curve (Reimer et al., 2013). The uncertainty of the calibrated ^{14}C age represents the 68% probability range. The onset of the Holocene in the Greenland NGRIP core, dated to 11,650 a BP (Walker et al., 2009), is used as wiggle match due to the distinct TOC increase in 642 cm depth of the Gemündener Maar core
15   (Fig. 2A, C and D). The Late Glacial to Holocene transition is commonly well recorded in maar sediments from the Eifel region, i.e. clear changes in deposition as well as pollen pattern, varve counted to 11,600 a BP in Lake Holzmaar (Zolitschka, 1998) and to 11,590 a BP in Lake Meerfelder Maar (Brauer et al., 1999; Litt et al., 2001, 2003; Litt and Stebich, 1999). Additionally, the clear appearance of *Corylus* Pollen in 620 cm depth (Fig. 2B; derived from
20   unpublished pollen analysis by F. Sirocko) was wiggle matched to the appearance of *Corylus* pollen in the adjacent Lake Holzmaar core, dated to 10,450 a BP (Sirocko et al., 2016). The beginning of the Younger Dryas period was set to 12,680 a BP (200 a after the Laacher See Tephra), according to the findings from Lake Meerfelder Maar (Litt et al., 2001). The investigated core section from 607 cm to 694 cm depth, with regard to the biomarkers, covers
25   the time between ~ 13,200 a and 9,700 a BP, i.e. the Allerød, Younger Dryas, Preboreal, and the beginning of the Boreal (Fig. 2C). Assuming a constant sedimentation rate between the markers results in an average resolution of 58 a/cm; the minimum and maximum resolution are 19 and 164 a/cm, respectively. The part above the Laacher See Tephra reveals a lower mean resolution (63 a/cm) than the section below (30 a/cm).

30

2.3 Biomarker and compound-specific isotope analysis

For δ^2H analyses of *n*-alkanes as well as $\delta^{18}O$ analyses of sugars, 59 samples were prepared from 607 cm to 694 cm depth of the Lake Gemündener Maar GM1 core (Fig. 3A and

Climate
of the Past
Discussions

B), in order to cover the core section with already high TOC content and the Late Glacial to Holocene transition (Fig. 2A, C and D). *n*-Alkanes were extracted from 1-6 g freeze-dried and grinded samples by microwave extraction at 100°C for 1 h, using 15 ml of solvent (dichloromethane and methanol, in a ratio 9:1). The resultant total lipid extracts were separated

5   over aminopropyl silica gel (Supelco 45 μm) filled pipette columns. Nonpolar compounds (including *n*-alkanes) were eluted with *n*-hexane. The fraction was spiked with a known amount of 5α-androstanone, used as internal standard. Identification and quantification was carried out on an Agilent MS 5975 (EI) interfaced with an Agilent 7890 GC equipped with a 30 m fused silica capillary column (HP5-MS 0.25 mm i.d., 0.25 μm film thickness), and a split/splitless

10   injector operating in splitless mode at 320°C. Carrier gas was helium and the temperature program was 1 min at 50°C, from 50 to 200°C at 30°C min^{-1}, from 200 to 320°C at 7°C min^{-1}, 5 min at 320°C. Data recording comprised the total ion count (scan mode from m/z 40 to m/z 600) and single ion monitoring (m/z 57, 71, 85 and 99). Concentrations were calculated relative to the internal standard and to an external standard (*n*-C_{21} to *n*-C_{40} alkane mixture, Supelco),

15   injected in different concentrations (40 ng/μl, 4 ng/μl, 1 ng/μl, 0.4 ng/μl).

       Prior to compound-specific isotope analyses, the *n*-alkanes were further purified. The nonpolar fractions were passed over a pipette column filled with activated $AgNO_3$ impregnated silica gel and a pipette column filled with zeolite (Geokleen). After drying, the zeolite was removed using hydrofluoric acid and the *n*-alkanes were recovered by liquid-liquid extraction

20   with hexane. The purified *n*-alkane fractions were measured for their compound-specific stable hydrogen isotope composition (δ^2H). The measurements were performed at the Institute of Geography, University of Bern on an IsoPrime 100 IRMS, coupled to an Agilent 7890A GC via a GC5 pyrolysis/combustion interface operating in pyrolysis modus with a Cr (ChromeHD) reactor at 1000°C. Samples were injected with a split/splitless injector. The GC was equipped

25   with 30 m fused silica column (HP5-MS, 0.32 mm inner diameter, 0.25 μm film thickness). The precision was checked by co-analyzing a standard alkane mixture (*n*-C_{27}, *n*-C_{29}, *n*-C_{33}) with known isotope composition (A. Schimmelmann, University of Indiana), injected twice every six runs. The samples were analyzed in threefold repetitions (except from the samples in 622 and 672 cm depth), and the analytical precision was generally better than 5‰. The stable

30   hydrogen isotope compositions are given in the δ-notation ($\delta^2H_{\text{n-alkane}}$) versus Vienna Standard Mean Ocean Water (VSMOW). The H_3^+-correction factor was checked every two days and stayed stable over the course of measurements at 3.14. The $\delta^2H_{\text{n-alkane}}$ values refer to the area weighted mean of the δ^2H values of *n*-alkanes with 27 and 29 carbon atoms (*n*-C_{27}, *n*-C_{29}), respectively, because of their relatively high abundance in the samples.

The sample preparation for $\delta^{18}O$ analyses of hemicellulose/polysaccharide-derived sugars followed standard procedures at the Institute of Agronomy and Nutritional Sciences, Soil Biogeochemistry, Martin-Luther-University Halle-Wittenberg, according the method of Zech and Glaser (2009). The monosaccharide sugars were hydrolytically extracted from

5   samples containing approximately 10 mg total organic carbon with 10 ml of 4 M trifluoroacetic acid at 105°C for 4 h, applying the method described by Amelung et al. (1996). After filtration over glass fibre filters, the extracted sugars were cleaned using XAD-7 (to remove humic-like substances) and Dowex 50WX8 columns (to remove interfering cations). Afterwards, the purified samples were freeze-dried and derivatized by adding methylboronic acid (4 mg in 400

10   µl pyridine) for 1 h at 60°C (Knapp, 1979). The methylboronic acid derivatization method ensures that the investigated pentoses arabinose and xylose as well as the deoxyhexoses fucose and rhamnose yield only one peak in the chromatograms (Gross and Glaser, 2004).

        The compound-specific $\delta^{18}O$ measurements were performed using a Trace GC 2000 coupled to a Delta V Advantage IRMS via an ^{18}O-pyrolysis reactor (GC IsoLink) and a ConFlo

15   IV interface (all devices from Thermo Fisher Scientific, Bremen, Germany). Each sample was measured in threefold repetition, embedded in-between co-derivatized sugar standards in various concentrations and known $\delta^{18}O$ values. The $\delta^{18}O$ values of the samples are expressed in δ-notation ($\delta^{18}O_{sugar}$) versus the Vienna Standard Mean Ocean Water (VSMOW). The measured $\delta^{18}O_{sugar}$ values were corrected for drift, amount and area dependency and also for

20   the hydrolytically introduced oxygen atoms that form carbonyl groups with the C1 atoms of the sugar molecules (Zech and Glaser, 2009). Mean standard uncertainties for the triplicate measurements of all 59 samples are 0.6‰, 0.7‰ and 0.7‰ for arabinose, fucose and xylose, respectively. The $\delta^{18}O_{sugar}$ values refer to the $\delta^{18}O$ values of the monosaccharides arabinose, fucose and xylose. Rhamnose areas, respectively concentrations, were too low for reliable

25   isotope measurements in many samples.

2.4 Conceptual framework for coupling $\delta^2H_{n\text{-alkane}}$ with $\delta^{18}O_{sugar}$ results

        The coupled $\delta^2H_{n\text{-alkane}}$-$\delta^{18}O_{sugar}$ approach was described in detail by Tuthorn et al. (2015) and Zech et al. (2013a). The most fundamental assumption of the approach is that the

30   isotope composition of leaf water can be reconstructed by applying biosynthetic fractionation factors on the measured $\delta^2H_{n\text{-alkane}}$ and $\delta^{18}O_{sugar}$ values (Fig. 4). The concept is furthermore based on the observation that isotope composition of global precipitation plots typically close to the global meteoric water line (GMWL; $\delta^2H_{prec} = 8 \cdot \delta^{18}O_{prec} + 10$; Dansgaard, 1964). In

Germany, a local meteoric water line (LMWL$_{Germany}$) slightly deviating from GMWL was described by Stumpp et al. (2014) (δ^2H$_{prec}$ = 7.72 ± 0.13 · δ^{18}O$_{prec}$ + 4.90 ± 0.01; Fig. 4), which we used as the baseline for our calculations. The quite similar LMWLs for Trier (δ^2H$_{prec}$ = 7.81 ± 0.08 · δ^{18}O$_{prec}$ + 5.06 ± 0.60) and Koblenz (δ^2H$_{prec}$ = 7.80 ± 0.07 · δ^{18}O$_{prec}$ + 2.68 ± 0.53) as

5   well as the GMWL are additionally displayed in Fig. 4 for comparison. The local precipitation is the source for soil water and shallow groundwater, which in turn acts as source water for plants. During daytime, however, leaf water is typically enriched compared to the source water due to evapotranspiration trough the stomata, plotting therefore right of the GMWL and the LMWLs (Fig. 4; Allison et al., 1985; Bariac et al., 1994; Walker and Brunel, 1990). The leaf

10   water reservoir at the evaporative sites achieves quickly steady-state conditions (Allison et al., 1985; Bariac et al., 1994; Gat et al., 2007; Walker and Brunel, 1990), meaning that the isotope composition of the transpired water vapor is equal to the isotope composition of the source water utilized by the plants during the transpiration process. The evaporative enrichment of leaf water under steady-state conditions, can be described via a Craig-Gordon model (e.g. Flanagan

15   et al., 1991; Roden and Ehleringer, 1999) by the following expression (e.g. Barbour et al., 2004):

$$\delta_e \approx \delta_s + \varepsilon^* + \varepsilon_k + (\delta_a - \delta_s - \varepsilon_k)\ \frac{e_a}{e_i}, \qquad\qquad\text{(Eq. 1)}$$

where δ_e, δ_s and δ_a are the hydrogen and oxygen isotope compositions of leaf water at the evaporative sites, source water and atmospheric water vapor, respectively, ε^* are the equilibrium enrichment expressed as $(1-1/\alpha_{L/V}) \cdot 10^3$ where $\alpha_{L/V}$ is the equilibrium fractionation

20   between liquid and vapor in ‰, ε_k are the kinetic fractionation parameters for water vapor diffusion from intracellular air space through the stomata and the boundary layer, both for ^{2}H and ^{18}O, respectively, and e_a/e_i is the ratio of atmospheric vapor pressure to intracellular vapor pressure. When leaf temperature is equal to air temperature, the e_a/e_i ratio represents the relative humidity of the local atmosphere (RH). If the plant source water and the local atmospheric

25   water vapor are in isotopic equilibrium, the term $\delta_a - \delta_s$ can approximated by $-\varepsilon^*$. Thus. Eq. (1) can be reduced to:

$$\delta_e \approx \delta_s + \left(\varepsilon^* + \varepsilon_k\right)(1 - \text{RH}). \qquad\qquad\text{(Eq. 2)}$$

The kinetic fractionation parameters (ε_k) are typically related to stomatal and boundary layer resistances with respect to water flux (Farquhar et al., 1989). Since direct measurements of those plant physiological parameters can be hardly assessed in a paleo application we used the

30   kinetic enrichment parameters C_k instead, derived from a more generalized form of the Craig-

Gordon model, for describing the kinetic isotope enrichment for ^{2}H and ^{18}O, respectively, which leads to Eq. (3) (Craig and Gordon, 1965; Gat and Bowser, 1991):

$$\delta_e \approx \delta_s + \left(\varepsilon^* + C_k\right)(1 - RH). \qquad \text{(Eq. 3)}$$

In a δ^2H-δ^{18}O diagram, the hydrogen and oxygen isotope composition of leaf and source water can be described as a local deuterium-excess (d) = δ^2H - 7.72 · δ^{18}O (Stumpp et al., 2014) in one equation by using the slope of the LMWL$_{Germany}$ (Eq. 4). This approach is comparable to the deuterium-excess definition from Dansgaard (1964), who used the equation d = δ^2H - 8 · δ^{18}O for a measure of the parallel deviation between a given point in the δ^2H-δ^{18}O diagram to the GMWL.

$$d_e \approx d_s + \left(\varepsilon_2^* - 7.72 \cdot \varepsilon_{18}^* + C_k^2 - 7.72 \cdot C_k^{18}\right)(1 - RH) \qquad \text{(Eq. 4)}$$

Where d_e and d_s are the deuterium-excess values of the leaf water at the evaporative sites and the source water, respectively, and the equilibrium (ε_2^* and ε_{18}^*) and kinetic enrichment parameters (C_k^2 and C_k^{18}) are expressed for both isotopes. From Eq. (1) to Eq. (4) the primary control of the relative humidity on the isotope composition of the leaf water is demonstrated when stomata are open through transpiration. If d_e can be derived from compound specific δ^2H and δ^{18}O measurements of the *n*-alkane and sugar biomarkers, which derive δ^2H$_e$ and δ^{18}O$_e$ values for the purpose of calculating d_e values via the equation $d_e = \delta^2$H$_e$ - 7.72 · δ^{18}O$_e$, and the d_s can be approximated also from the deuterium-excess of the LMWL$_{Germany}$ (= 4.9). Accordingly, Eq. (4) can be rearranged in order to calculate relative humidity of the local atmosphere normalized to leaf temperature as given by Eq. (5) (Hepp et al., 2017; Tuthorn et al., 2015; Zech et al., 2013a):

$$RH \approx 1 - \frac{\Delta d}{\left(\varepsilon_2^* - 7.72 \cdot \varepsilon_{18}^* + C_k^2 - 7.72 \cdot C_k^{18}\right)}, \qquad \text{(Eq. 5)}$$

where Δd is the distance between d_e and d_s, calculated as $\Delta d = d_e - d_s$. Equilibrium fractionation parameters (ε_2^* and ε_{18}^*) are derived from empirical equations of Horita and Wesolowski (1994) with mean daytime growth-period temperature of 14.8°C (from 6 a.m. to 7 p.m. and April to October, derived from the Nürburg-Barweiler station, approx. 25 km northeast of Lake GM; hourly data from 1995 to 2015 from Deutscher Wetterdienst, 2016). Equilibrium fractionation factors equal 83.8 and 10.15‰ for ^{2}H and ^{18}O, respectively. The kinetic fractionation parameters (C_k^2 and C_k^{18}) for ^{2}H and ^{18}O are set to 25.1 and 28.5‰, respectively, according to Merlivat (1978), who reported maximum values during the molecular diffusion process of water through a stagnant boundary layer. The assumption that maximum kinetic fractionation occurs seems to be most suitable for sedimentological application where a signal averaging over

decades can be assumed (see above and discussion in Zech et al., 2013a). It should be also noted that ε_k values of broadleaf trees and shrubs over broad climatic conditions are well in the range with used C_k^2 and C_k^{18} values, revealing 23.9 (± 0.9) and 26.7‰ (± 1.0) for $\delta^2 H$ and $\delta^{18}O$, respectively (derived from supplementary data of Cernusak et al., 2016).

5   The nominator of Eq. (5) describes the parallel distance between the deuterium-excesses of LMWL and leaf water at the evaporative sites which is converted into relative humidity values, while the denominator is a combination of the slopes of LMWL and LEL. This means in turn that the quantification with Eq. (5) is done by obtaining the distance between the source water points, calculated via the intersects between the individual local evaporation lines and the

10   LMWL$_{Germany}$, and the leaf water points. The underlying slope of those LELs can be derived from Eq. (6) via the Craig-Gordon model using the same assumptions as outlined above in a rearranged form (Eq. 6; Zech et al., 2013a). When using the fractionation parameters from above, the slope of the LEL is constant over time, independent from RH and equal to ~ 2.8 (Eq. 6).

$$S_{LEL} = \frac{\delta_e^2 - \delta_s^2}{\delta_e^{18} - \delta_s^{18}} \approx \frac{\varepsilon_2^* + C_k^2}{\varepsilon_{18}^* + C_k^{18}} \qquad \text{(Eq. 6)}$$

15   In order to provide an uncertainty interval in terms of measurement precision covering the Lake Gemündener Maar relative humidity record, pooled standard errors (SE) of d_e values were used (according to Eq. 7) to generate maximum and minimum values for Eq. (5), which result in a lower and upper relative humidity limit.

$$SE\ d_e = \sqrt{\left(SE\ \delta^2 H_{n\text{-alkane}}\right)^2 + 7.72 \cdot \left(SE\ \delta^{18}O_{sugar}\right)^2} \qquad \text{(Eq. 7)}$$

20   **2.5 Monte-Carlo-based correlation analysis**

In order to account for uncertainties regarding the here established Lake Gemündener Maar Late Glacial to Early Holocene age-depth model (cf. section 2.2), we applied a Monte-Carlo-based correlation analysis to compare more robustly our RH$_{dv}$ record with the IntCal13 ^{14}C production rates (data from Muscheler et al., 2014). This is assessed by varying the onset

25   of *Corylus*, the onset of the Holocene and the charcoal ^{14}C age of the Lake Gemündener Maar core. The Laacher See Tephra is accurately varve counted with an error of ± 40 a (Brauer et al., 1999), which is negligible small compared to the others, and therefore excluded from the variation procedure. The onset of *Corylus* pollen is dated to 10,450 a BP in ~ 8.4 m depth

Climate
of the Past

Discussions

Open Access

EGU

(Sirocko et al., 2016) in the adjacent Lake Holzmaar core. To put an error on this date, four ^{14}C ages derived from twig material of Lake Holzmaar core are used (from the supplements of Sirocko et al. 2013) two above the *Corylus* onset (4.8 m depth: 3560 ± 25 and 3615 ± 30 a BP) and two below (8.5 m depth: 9740 ± 140 and 9670 ± 90 a BP). By using the CalPal-software

5 (Weninger and Jöris, 2008) with the IntCal13 calibration curve (Reimer et al., 2013) these ages were calibrated to 3860 ± 30, 3930 ± 40, 11080 ± 220 and 11000 ± 160 a cal BP. The errors of the calibrated ^{14}C ages refer to the 68% probability range. This gives a mean error for the upper dates of ± 35 a, and ± 190 a for the lower ones. In error propagation we combined both mean errors to ± 225 a for the onset of *Corylus* pollen in the Lake Gemündener Maar core. For the

10 onset of the Holocene in the Lake Gemündener Maar sediments, which was defined as wiggle match between the TOC increase in 642 cm depth and the onset of the Holocene in the Greenland NGRIP core (dated to 11,650 a BP Walker et al., 2009), we combined the maximum counting error for the Holocene onset in the NGRIP core of ± 99 a (Walker et al., 2009) together with a potential time lag of 170 a (Rach et al., 2014) to ± 269 a. Such a time lag was detected

15 in sedimentary hydrogen isotope values of aquatic and terrestrial *n*-alkanes from Lake Meerfelder Maar concerning a lag in hydrologic and environmental effects in Western Europe occurring 170 a later compared to Greenland cooling at the GI-1 to GS-1 transition (Rach et al., 2014). Finally, the derived errors for the onset of the Holocene (±269 a), the onset of *Corylus* (±225 a) and the calibrated charcoal ^{14}C age (±110 a) were used in a correlation procedure based

20 on a Monte-Carlo-Simulations (realized in R, version 3.2.2, R Core Team, 2015). In a first mode the time steps were set to 5 a, while the refining, 10 a around the highest correlation coefficient, was done in yearly resolution. This procedure allows deriving optimized ages for those three dates, which in turn enables the calculation of an adjusted age-depth model.

25 **3 Results & Discussion**

3.1 Source identification of bulk organic matter and of the investigated *n*-alkane and sugar biomarkers

For basic sedimentological characterization, measurements of TC and TOC (both Fig. 2D), TN (Fig. 2E), δ^{15}N (Fig. 2F), $\delta^{13}C_{TC}$ and $\delta^{13}C_{TOC}$ (both Fig. 2G) as well as the TOC/TN

30 ratio (Fig. 2H) are displayed from 605 cm to 727 cm depth. TC and TOC values range from 0.6 to 20.7% and from 0.6 to 19.7%, respectively. Slightly higher TC values compared to TOC can be attributed to the occurrence of carbonate. TN reveals a range of 0.1 to 1.4%. In general, TOC and TN depth profiles show the same trends (TOC vs. TN: r = 0.99, p < 0.001, n = 110), i.e. an increase during the Allerød, lower values during the Younger Dryas, and larger variations

during the Preboreal and the Boreal. The $\delta^{15}N$ values range from 0 to 5‰, showing the maximum and minimum within the Allerød period. $\delta^{13}C_{TC}$ and $\delta^{13}C_{TOC}$ reveal values between -31 to -17‰ and -36 to -24‰, respectively. While $\delta^{13}C_{TC}$ show maximum values in 703 cm depth, $\delta^{13}C_{TOC}$ is decreasing continuously from the beginning to the end of the Allerød,

5 followed by increasing values during the Younger Dryas and the Preboreal/Boreal, interrupted by a short decrease around the beginning of the Holocene. $\delta^{13}C_{TC}$ clearly show the presence of carbonate between 690 cm and 727 cm depth, due to the more positive $\delta^{13}C_{TC}$ values compared to $\delta^{13}C_{TOC}$ values, which is however not clear noticeable from the difference between TC and TOC (compare Fig. 2G with 2D). TOC/TN ratios range from 5 to 16 with the end of the Allerød

10 revealing increasing ratios, while the late Younger Dryas shows slightly decreasing ratios and the Preboreal is marked by the highest ratios.

(Fig. 2)

The source of organic matter in lacustrine sediments of small lakes, as one of the most crucial questions and challenges when interpreting organic proxies from lacustrine sedimentary

15 records (Meyers and Ishiwatari, 1993), can either be autochthon (aquatic origin) or allochthon (terrestrial origin). The carbon to nitrogen ratio (C/N) and $\delta^{13}C$ values are most common proxies for sedimentary source determination. While non-vascular aquatic organisms often reveal C/N ratios between 4 and 10 (due to low amounts of cellulose and lignin), vascular plants show commonly C/N ratios of 20 and higher (Meyers and Ishiwatari, 1993). Already Prahl et al.

20 (1980) used a C/N ratio of > 12 as threshold for a dominance of terrestrial input (Fig. 2H). The Lake Gemündener Maar samples below 642 cm (onset of the Holocene) show TOC/TN ratios of mostly < 12, pointing to a high aquatic input, whereas in the section above the ratios shift to values > 12, suggesting a partial contribution of terrestrial material (Fig. 2H; Meyers and Ishiwatari, 1993). Lake Gemündener Maar $\delta^{13}C_{TOC}$ values (Fig. 2G) are well in range with C3

25 land plants and lacustrine algae (Meyers and Lallier-Vergés, 1999). Most likely, no changes between C3 and C4 land plants occurred in Lake Gemündener Maar catchment history, due to the absence of C4 land plants. Thus, no clear additional information about the sedimentary organic matter origin in Lake Gemündener Maar sediments can be achieved neither by $\delta^{13}C_{TOC}$ alone (Lücke et al., 2003), nor by combining $\delta^{13}C_{TOC}$ with TOC/TN ratios (Meyers and Lallier-

30 Vergés, 1999). When considering that both $\delta^{13}C_{TOC}$ and C/N values of terrestrial organic matter are additionally affected by mineralization and degradation, resulting in more positive $\delta^{13}C_{TOC}$ values and lower C/N ratios (e.g. Zech et al., 2007), a straightforward interpretation of those proxies seems to be challenging. Much less common, $\delta^{15}N$ values are used to derive information about sedimentary organic matter origin (Meyers and Ishiwatari, 1993). Source determination

using ^{15}N is based on the finding that dissolved nitrate, which is the nitrogen source for aquatic plants, and atmospheric nitrogen, which is the nitrogen source for land plants, largely differ in their isotope ratios (Peterson et al., 1985). For Lake Gemündener Maar, δ^{15}N values (Fig. 2F) imply more aquatic input below 690 cm depth while above stronger terrestrial imprint is

5   obvious which is in principle resembling the TOC/TN record. However, numerous alternation pathways of sedimentary ^{15}N due to biogeochemical processes, like nitrogen uptake by plants, various nitrogen sources, discrimination during denitrification, and diagenesis, complicate the use of δ^{15}N as direct source determination proxy (Altabet et al., 1995; Meyers and Lallier-Vergés, 1999; Wolfe et al., 1999). However, the δ^{15}N peak in 690 cm depth coincides with a

10   striking brownish layer (Fig. 2A), revealing low C/N ratios. Possible this marks the input of soil material from the catchment, with soils typically being more positive in δ^{15}N compared to plant material (Natelhoffer and Fry, 1988). Since the origin of the sedimentary organic matter cannot be determined exactly, the Lake Gemündener Maar sedimentary TOC values (Fig. 2D) should also not be over interpreted. Higher TOC contents during the Allerød, Preboreal and

15   Boreal are typically linked to warmer conditions favorable for aquatic biomass production, whereas the lower TOC values during the Younger Dryas are associated with colder and dryer climate with increasing minerogenic sedimentation (e.g. Brauer et al., 1999). Still, the low TOC content during the late Allerød section (below 690 cm) of Lake Gemündener Maar point to a low organic matter production in the lake as well as allochtonous organic matter input. Also the

20   Allerød sediments of Lake Holzmaar are not characterized by TOC maxima (Lücke et al., 2003).

Despite the uncertainties describing the source of the bulk sedimentary organic matter in Lake Gemündener Maar sediments using bulk characteristics, the origin of the sedimentary biomarkers, namely *n*-alkanes and sugars, needs to be addressed. This is important because

25   aquatic biomarkers incorporate the isotope composition of lake water, while terrestrial biomarkers incorporate the isotope composition of leaf water (Huang et al., 2004; Kahmen et al., 2013a; Mügler et al., 2008; Sachse et al., 2004, 2012; Sauer et al., 2001; Tuthorn et al., 2014; Zech et al., 2013b, 2014b). For a successful application of the coupled δ^2H$_{n\text{-alkane}}$-δ^{18}O$_{sugar}$ approach, in terms of deriving relative humidity values, the biomarkers have to originate from

30   leaf material of higher terrestrial plants (Hepp et al., 2017; Tuthorn et al., 2015; Zech et al., 2013a). Regarding the *n*-alkane biomarker, high amounts of the chain lengths *n*-C$_{27}$ and *n*-C$_{29}$ were detected in the Lake Gemündener Maar sediments, which enables then robust compound-specific δ^2H measurements afterwards. Those homologues originate typically from epicuticular leaf wax layers of higher terrestrial plants in the catchment (e.g. Eglinton and Hamilton, 1967).

The investigated sugar biomarker pattern were previously studied by Hepp et al. (2016), showing that arabinose is primarily of terrestrial origin (higher vascular plants), whereas fucose and xylose are mostly of aquatic origin (algae). This interpretation was in agreement with (paleo)soil and sediment data compiled from the literature (cf. references in Hepp et al., 2016).

5   Finally, it should be clarified if the investigated sedimentary biomarkers are primarily of leaf origin from higher plants in the catchment. While this holds most likely true for the investigated n-alkanes, due to their primary source from epicuticular leaf wax layers of higher terrestrial plants, the neutral sugar arabinose is found in leaf, stem and moss material (Jia et al., 2008; Prietzel et al., 2013; Zech et al., 2012, 2014b). Firstly, high coverage of the catchment
10   by trees is obvious (Fig. 1C), leading to high degree of leaf litter input in autumn. Secondly, vegetation grown on the maar crater wall is supposed to be the main input of biomass into the lake, which is typical for steeply shored mare lakes, while the shoreline vegetation contribution should be comparable small. Thirdly, an arboreal to nonarboreal pollen ratio of ~ 84, as mean value throughout the investigated core section is reported (derived from unpublished pollen
15   analysis by F. Sirocko). We therefore assume that arabinose, as well as n-C$_{27}$ and n-C$_{29}$, originate primarily from hemicellulose structures and from epicuticular waxes of tree leaf material, respectively.

3.2 Reconstructing leaf water isotope composition based on $\delta^2H_{n\text{-alkane}}$ and
20    $\delta^{18}O_{sugar}$

The δ^2H depth profiles reveal variations of -222 to -134‰ and -220 to -147‰ for n-C$_{27}$ and n-C$_{29}$, respectively (Fig. 3A). Their δ^2H patterns correlate highly significant with each other (r = 0.7, p < 0.001, n = 59). Weighted mean δ^2H values were calculated using the relative amounts of n-C$_{27}$ and n-C$_{29}$. More negative δ^2H values are obvious during the Younger Dryas
25   (~ 17‰ more negative, with a mean of -194‰), compared to the Allerød (-182‰), Preboreal (-178‰) and Boreal (-171‰), with regard to the weighted mean n-alkane depth profile. Overall the Holocene part of the core average at ~ -175‰, where consistently also largest fluctuations are observed (~50‰). The $\delta^{18}O$ values for arabinose, xylose and fucose range from 28 to 41‰, 26 to 45‰ and 27 to 46‰, respectively (Fig. 3B). They overall reveal similar trends (arabinose
30   vs. xylose: r = 0.7, p < 0.001, n = 59; arabinose vs. fucose: r = 0.8, p < 0.001, n = 59; xylose vs. fucose: r = 0.8, p < 0.001, n = 59). All sugar records show a clear shift to more positive values at the Younger Dryas to Holocene transition. While xylose and fucose exhibit a change of ~ 8 and 6‰, arabinose $\delta^{18}O$ values show a less positive shift of ~ 3‰ (changes are based on the

mean $\delta^{18}O$ values for the Younger Dryas compared to the Preboreal/Boreal period). Xylose is however slightly more negative throughout the Allerød and Younger Dryas compared to arabinose and fucose. Consistently less pronounced changes can be observed for the Allerød-Younger Dryas transition of 1.8, 1.4 and 0.5‰ for xylose, fucose and arabinose, respectively (based on the mean $\delta^{18}O$ values for the Allerød compared to the Younger Dryas). A distinct minimum during the early Preboreal (633 cm depth) characterizes all three $\delta^{18}O$ sugar records.

(Fig. 3)

When applying the $\delta^2H_{n\text{-alkane}}$-$\delta^{18}O_{sugar}$ paleohygrometer approach to lacustrine sediments, not only the basic origins of the sedimentary biomarkers have to be clarified (cf. section 3.1), but also prerequisite that leaf water isotope composition is recorded in the biomarkers and can thus be reconstructed from them. The isotope composition of leaf wax n-alkanes and leaf (hemi-)celluloses from higher plants are known to be strongly related to the water in which they are biosynthesized. They reflect basically the isotope composition of leaf water during photosynthetic activity (Barbour and Farquhar, 2000; Cernusak et al., 2005; Kahmen et al., 2013a; Sachse et al., 2012). Hence, the isotope signature of the paleo leaf water, $\delta^{18}O_l$ and δ^2H_l, respectively, can be reconstructed by using known biosynthetic fractionation factors (Fig. 4; Eq. 8 and 9). For this purpose, fractionation factors of -160‰ for ^2H of alkanes n-C_{27} and n-C_{29} (ε^2_{bio}; Sachse et al., 2012; Sessions et al., 1999), and $+27$‰ for ^{18}O of hemicellulose sugar arabinose (ε^{18}_{bio}; Cernusak et al., 2003; Schmidt et al., 2001; Sternberg et al., 1986; Yakir and DeNiro, 1990) are assumed.

$$\delta^{18}O_l = (\delta^{18}O_{arabinose} - \varepsilon^{18}_{bio})/(1 + \varepsilon^{18}_{bio}/1000) \qquad (Eq. 8)$$

$$\delta^2H_l = (\delta^2H_{n\text{-alkane}} - \varepsilon^2_{bio})/(1 + \varepsilon^2_{bio}/1000) \qquad (Eq. 9)$$

Sucrose exported from photosynthesizing leaves was shown to be ~ $+27$‰ more positive compared to leaf water (e.g. Cernusak et al., 2003). However, also the cellulose biosynthesis is associated with an enrichment of ~ $+27$‰ compared to the synthesis water, as shown in growth experiments (e.g. Sternberg et al., 1986; Yakir and DeNiro, 1990). This means that the isotope signal from the leaf water incorporated in the transport sugar sucrose can be dampened by oxygen exchange with local synthesis water during (hemi-)cellulose biosynthesis in the sink tissue (e.g. Barbour and Farquhar, 2000). Barbour and Farquhar (2000) related this signal damping to the proportion of unenriched source water contributing to the local synthesis water (p_x) and to the proportion of exchangeable oxygen during cellulose synthesis (p_{ex}). Latter is often assumed to be rather constant around 0.40, as estimated from leaf and wood cellulose of *Eucalyptus globulus* and values compiled from literature (Cernusak et al., 2005), meaning

that 40% of the oxygens in the stem cellulose exchanged. Indeed, studies on leaf material of *Eucalyptus globulus* (Cernusak et al., 2005) and for *Gossypium hirsutum* (Barbour and Farquhar, 2000) report a total damping of 38% during leaf cellulose synthesis. However, already Wang et al. (1998) presented a large range of damping between 4 and 100% for leaf

5   cellulose synthesis (provided in the supplementary material of Cheesman and Cernusak, 2017), based on plant data grown under the same conditions at Jerusalem Botanical Gardens. The signal damping depends also on p_x. Since no direct p_x measurements on dicotyledonous plant leaves are available so far (Liu et al., 2017), no clear conclusion can be drawn about the oxygen signal damping during (hemi-)cellulose synthesis in the leaves of dicotyledonous plants. The

10   signal damping effect described for cellulose synthesis, however, could partially be lost during synthesis of leaf hemicellulose structures. Pentoses, like the hemicellulose-derived arabinose, are biosynthesized via decarboxylation of the carbon at position six (C6) from glucose (Altermatt and Neish, 1956; Burget et al., 2003; Harper and Bar-Peled, 2002). Waterhouse et al. (2013) showed that the oxygens at C6 position in glucose moieties are most strongly affected

15   by the exchange with local water medium of 80%, as indicated by heterotrophic cellulose synthesis. This leads to the approximation that the influence of the source water and the respective oxygen exchange can be considered negligible for leaf arabinose from trees. This is supported by a strong relationship between leaf water and leaf hemicellulose $\delta^{18}O$ values of dicotyledonous plants grown in climate chambers, pointing to a strong incorporation of the leaf

20   water signal into the leaf hemicellulose sugars (Hepp et al., 2018). The reduction of the signal damping does not seem to apply for the respective stem hemicelluloses, with a mean ^{18}O signal damping of ~ 66% (Sternberg, 2014; Zech et al., 2014c) For a C_4 grass *Cleistogenes squarrosa*, Liu et al. (2016) presented a signal damping range between 34 and 53%. Direct p_x measurements in the grass leaf growth-and-differentiation zone of the same C_4 grass reveal

25   values between 0.9 and 1.0 for ^{18}O (Liu et al., 2017). Comparison of grasses to the tree stem regarding the signal transfer from leaf water into the (hemi-)cellulose was already reported by Helliker and Ehleringer (2002). A correction seems to be required against the background of *Poaceae* pollen concentrations between 11 and 33% during the Allerød and Younger Dryas periods in Lake Gemündener Maar sediments (Fig. 3C; derived from unpublished pollen

30   analysis by F. Sirocko). A correction procedure based on mass balance considerations is given in Eq. (10) in order to adjust $\delta^{18}O_l$ to $\delta^{18}O_l{}^{\#}$:

$$\delta^{18}O_l{}^{\#} = \{(\delta^{18}O_l - \delta^{18}O_s)/[f_{non\text{-}grasses} + (1 - 0.4) - f_{non\text{-}grasses} \cdot (1 - 0.4)]\} + \delta^{18}O_s. \qquad \text{(Eq. 10)}$$

The correction presented in Eq. (10) is based on assumptions that 40% (0.4) of the leaf water enrichment is lost during hemicellulose biosynthesis of grass leaves, which is well in range with

Climate
of the Past
Discussions

values presented in the literature for cellulose synthesis in tree rings and grasses, respectively (Cernusak et al., 2005; Liu et al., 2016). Furthermore, the *Poaceae* pollen concentration in percentage is used to calculate the fraction of non-grassy pollen [$f_{non-grasses}$ = (100 − *Poaceae*)/100] corresponding to the non-grassy biomarker contribution, which may serve as

5   rough approximation. For a paleo application, $\delta^{18}O_s$ remains a priori unknown. Therefore, the intercept between the individual LEL´s (Eq. 6) and the LMWL of Germany were used to generate $\delta^{18}O_s$ values. The overall assumption is still that (hemi-)cellulose is solely biosynthesized from immediate products of photosynthesis. Storage substances like starch indeed contribute to leaf cellulose synthesis (Terwilliger et al., 2001). So far it can only be

10   speculated that this does not significantly influence the strong relationship between (hemi-)cellulose and leaf water (Terwilliger et al., 2002), as appropriate studies are lacking. Leaf water inhomogeneity and sucrose synthesis gradients within leaves could weaken the leaf water to (hemi-)cellulose correlation (Lehmann et al., 2017; Santrucek et al., 2007). Additionally, changes in ^{18}O fractionation (ε^{18}_{bio}) could hamper a robust leaf water reconstruction based on

15   leaf hemicellulose. Sternberg and Ellsworth (2011) showed for heterotrophically generated cellulose a strong temperature dependence of the biosynthetic fractionation factor. A temperature dependency was also found for ε^{18}_{bio} of stem hemicelluloses from dicotyledonous plants, recalculated by Sternberg (2014) based on results from Zech et al. (2014a). In the reply the authors show that rather the ^{18}O leaf water signal damping (p_{ex}), associated with the steam

20   hemicelluloses synthesis, can be related to the temperature growth (Zech et al., 2014c). However, the evaluation of leaf material from the same plants strongly suggests an ^{18}O fractionation factor of around +27‰ (Hepp et al., 2018). This confirms the validity of Eq. (8) in order to derive leaf water from arabinose $\delta^{18}O$ values.

The climate chamber experiment of Hepp et al. (2018) revealed furthermore a ^2H

25   fractionation between long chained *n*-alkanes (*n*-C_{29} and *n*-C_{31}) and leaf water around -156‰. This is well in line with the commonly reported −160‰ (Sachse et al., 2012; Sessions et al., 1999) and is confirmed by climate chamber studies of dicotyledonous plants (Kahmen et al., 2011b, 2013a; Tipple et al., 2015). However, the latter studies reveal also a range of ~ 35‰, interpreted as species-specific effects during *n*-alkane biosynthesis. Much more pronounced is

30   the difference between dicotyledonous and monocotyledonous C_3 plants regarding the degree to which the leaf water isotope enrichment is transferred into leaf *n*-alkanes (Gamarra et al., 2016; Kahmen et al., 2013a). While dicotyledonous plants show signal transfer rates of 96% on average (Kahmen et al., 2013a), a larger range between 38 and 61% are found for monocotyledonous plants (Gamarra et al., 2016). The latter imply that 39 to 62% of the ^2H leaf

water enrichment is not recorded by the *n*-alkanes of grasses. The outlined discussion lead to the conclusion that $\delta^2 H_l$ can be reconstructed based on $\delta^2 H_{n\text{-alkane}}$ values (using $\delta^2 H$ of *n*-C$_{27}$ and *n*-C$_{29}$ via Eq. 9). However, a correction seems to be required for grass *n*-alkane input, equivalent to Eq. (10):

$$\delta^2 H_l^{\#} = \{(\delta^2 H_l - \delta^2 H_s)/[f_{non\text{-}grasses} + (1 - 0.5) - f_{non\text{-}grasses} \cdot (1 - 0.5)]\} + \delta^2 H_s, \qquad \text{(Eq. 11)}$$

5   where $\delta^2 H_l^*$ are the grass corrected $\delta^2 H_l$ values. The $\delta^2 H_s$ values and the non-grassy pollen fraction are defined as in Eq. (10). The mass balance correction presented in Eq. (11) is based on assumptions that only 50% of the leaf water enrichment is incorporated by the *n*-alkanes during biosynthesis in grass leaves (based on a mean value calculated from values reported by Gamarra et al., 2016). Besides the discussion about correct and constant biosynthetic

10   fractionation factors and signal damping factors during biosynthesis, the uncorrected $\delta^2 H$ values of *n*-C$_{27}$ and *n*-C$_{29}$ can be compared to $\delta^2 H$ results from *n*-C$_{29}$ alkanes extracted from close-by Meerfelder Maar sediments (Rach et al., 2014). This record covers a comparable timespan from 13,100 to 11,000 varve a BP. The Lake Gemündener Maar $\delta^2 H_{n\text{-alkane}}$ record resembles the previously presented Lake Meerfelder Maar results with an overall range of 75‰ (13,200 to

15   9,700 a BP), with ~ -8‰ more negative values in mean during the Younger Dryas compared to the Allerød and a ~ +17‰ shift in average from Younger Dryas to Holocene. The Lake Meerfelder Maar $\delta^2 H$ *n*-C$_{29}$ values, interpreted as reflecting mainly $\delta^2 H$ composition of paleo leaf water, reveal a range of 68‰, ~ -8‰ more negative values in mean during the Younger Dryas compared to the Allerød and a Younger Dryas to Holocene shift in average of ~ +19‰

20   (Rach et al., 2014).

In summary, the above outlined discussion results in four different leaf water correction scenarios as input for Eq. (5) (Tab. 1).

(Tab. 1)

25   **3.3 Reconstructing relative humidity based on the coupled $\delta^2 H_{n\text{-alkane}}$-$\delta^{18} O_{sugar}$ paleohygrometer approach**

The biomarker-based leaf water values ($\delta_l = \delta^2 H_l$, $\delta^{18} O_l$ via Eq. 8 and 9) result in deuterium-excess values of leaf water (d_l), which range between -125 and -30‰ (Fig. 4 and 5A). A clear enrichment is observed compared to the source water signal (d_s), which was set to

30   +4.9‰ as derived from the deuterium-excess of the LMWL$_{Germany}$ (cf. section 2.4; Fig. 4).

(Fig 4)

Using d_l values (and d_s) as input for Eq. (5), relative humidity values during daytime and vegetation period (RH_{dv}) can be calculated (scenario 1 in Tab. 1). Reconstructed RH_{dv} values reveal a range from 32 to 82% (Fig. 5B). The error bars covering the Lake Gemündener Maar RH_{dv} record, calculated using pooled d_e standard errors ranging from 3.2 to 44.4‰ according

5   Eq. (7), results in a span of 1.7 to 23.4% in relative humidity terms. It should be noted that for two data points (622 and 672 cm depth) only one, instead of three, $\delta^2H_{n\text{-alkane}}$ measurement result is available, avoiding the calculation of pooled d_e standard errors for those. However, these two data points were excluded from the ranges given above. The RH_{dv} record shows distinctly lower relative humidity values during the late Younger Dryas period, early and late

10   Preboreal, while the Allerød, first half of the Younger Dryas, middle Preboreal and the Boreal are characterized by more humid conditions. The plausibility of the reconstructed RH_{dv} values is furthermore confirmed by the comparison to modern RH_{dv} values from the adjacent meteorological station Nürburg-Barweiler (approx. 25 km northeast of Lake GM; Fig. 5C). Mean reconstructed RH_{dv} values (mean RH_{dv} = 53%; mean RH_{dv} upper limit = 46%; mean RH_{dv}

15   lower limit = 61%) resembles the modern mean vegetation period (growth time; April to October) daytime (6 a.m. to 7 p.m.) humidity value of 67% (hourly data from 1995 to 2015 from Deutscher Wetterdienst, 2016). In addition, the range of the reconstructed RH_{dv} values of 50% is well in agreement with in modern RH_{dv} variability of 45%, within a range of 48% to 93% (definition and meteorological station details as above). The availability of Lake

20   Gemündener Maar *Poaceae* pollen concentrations (Fig. 3C and 5C; derived from unpublished pollen analysis by F. Sirocko) enables calculating three correction leaf water scenarios, which take into account that grass-derived biomarkers are typically less sensitive leaf water recorders (scenarios 2-4 in Tab. 1; cf. 3.2). The effects on the deuterium-excess of leaf water as well as on the corresponding relative humidity values are shown in Fig. 5A and B.

25   (Fig. 5)

More specifically, the full correction for grass-derived biomarker contribution (scenario 4 in Tab. 1) result in 0.0 to -6.2 (mean -1.9%) when comparing RH_{dv} to $RH_{dv}^{\#}{}^{*}$. The corresponding $d_l^{\#}{}^{*}$ value changes range between -11.8 and -0.1‰. Such small changes are still far below the pooled standard error introduced by the measurement errors (Fig. 5A and B). When only grass-

30   corrected arabinose-based $\delta^{18}O_l^{\#}$ values are used, whereas the *n*-alkane δ^2H_l input stays uncorrected (scenario 3 in Tab. 1), a range of -22.2 to -0.1‰ can be obtained in the $d_l^{\#}$ value differences, and the corresponding relative humidity value changes range between -0.1 and -11.6%, in terms of comparing RH_{dv} to $RH_{dv}^{\#}$. The opposite scenario became obvious when just the *n*-alkane based grass corrected $\delta^2H_l^{*}$ values are used to calculate relative humidity values

while arabinose based $\delta^{18}O_l$ remains uncorrected (scenario 2 in Tab. 1). This lead to shifts of 0.0 to 5.5%, when comparing RH_{dv} to $RH_{dv}*$. Indeed, the respective positive d_l* value changes of 0.1 to 10.4‰ are strongly associated to the *Poaceae* pollen concentration. It is therefore clear why the full corrected $RH_{dv}^{\#}*$ values differ only minimal from the uncorrected RH_{dv}. Based on that finding, it could be argued that RH_{dv} values derived from δ^2H_l and $\delta^{18}O_l$ are relatively robust against grassy biomarker contributions. Further implications against a correction arose from the fact that the relative humidity values derived from the coupled $\delta^2H_{n\text{-alkane}}$-$\delta^{18}O_{sugar}$ approach are interpreted as reflecting daytime and vegetation period relative humidity (RH_{dv}; Tuthorn et al., 2015). Leaf biomass production in a temperate forest reveals a bimodal distribution regarding the height due to a dense understory vegetation and high leaf production of annually deciduous trees at ground and upper canopy level, respectively (Graham et al., 2014). Moreover, strong gradients in relative humidity can occur in temperate forest ranging from near to saturated conditions (> 95%) close to the ground (< 5 m height) and highly unsaturated conditions (down to ~ 60%) throughout the upper part of the forest (> 5 m height) in a diurnal cycle (Parker, 1995). This suggest that tree leaves are in average build up under lower humidity conditions, compared to the understory (leaf) biomass. With regard to grass-derived *n*-alkane and sugar contributions to the Lake Gemündener Maar δ^2H and $\delta^{18}O$ biomarker records below 642 cm depth, this would suggest a higher impact of the more humid understory signal, what could lead to higher reconstructed relative humidity values when *Poaceae* input is high. This would contradict the applied grass correction (Eq. 10 and 11), which should therefore be even more carefully reviewed in order to avoid an over interpretation of the corrected values.

It is widely accepted that the bulk leaf water is less enriched compared to the leaf water at the evaporative sites (e.g. Allison et al., 1985; Barbour, 2007). Furthermore the simplified Craig-Gordon model to derive RH values (Eq. 5) requires per definition the input of the deuterium-excess of evaporative site leaf water, as outlined in section 2.4 (Flanagan et al., 1991; Roden and Ehleringer, 1999). In order to estimate the effect on the deuterium-excess of differences between Craig-Gordon predicted δ_e (evaporative site leaf water) and measured δ_l (bulk leaf water), deuterium-excess (d_l and d_e) values were calculated for broadleaf trees and shrubs using the supplementary dataset of Cernusak et al. (2016). Using the complete leaf water isotope data of that supplements, which are available for Australia (Kahmen et al., 2013b) and Hawaii (Kahmen et al., 2011a), a deuterium-excess formulation of $d = \delta^2H - 6.86 \cdot \delta^{18}O$, based on the additional available xylem water isotope data, was found. The thus calculated values average at -88.5 (±35) and -79.6‰ (±29) for d_l and d_e, respectively. This means that in this

Climate
of the Past

Open Access

Discussions

EGU

dataset, d_l is in average 8.9‰ more negative than d_e, with a standard deviation of 16‰. Since it is general accepted that δ_e is more positive compared to δ_l, one would expect d_e to be more negative compared to d_l. Illustrated in a δ^2H-$\delta^{18}O$ diagram, the δ_e should plot further right on a LEL, while the δ_l is assumed to be a mixture plotting therefore closer to the source water, still on the LEL. However, the average difference is still smaller than the mean analytical error of biomarker-derived d_l with 15‰ (see Eq. 7 for calculation). A deuterium-excess correction to account for the difference between d_l and d_e seems therefore not crucial.

For a successful relative humidity reconstruction, a constant LEL slope is assumed, meaning isotopic equilibrium between plant source water and the local atmospheric water vapor. For giving a estimation weather this assumption is valid here, one should distinguish between isotopic equilibrium between local atmospheric water vapour and local precipitation and that between local atmospheric water vapour and local source water available for plants, while latter is of importance here. Under present-day European climate, close to isotope equilibrium conditions at ground-level temperature between monthly precipitation and atmospheric water vapour can be assumed (Araguás-Araguás et al., 2000; Jacob and Sonntag, 1991), with the exception of snow during winter months (snow preserves isotope signature established high in the clouds, at significantly lower temperatures). However, the source water for plants is mostly a mixture between soil water and shallow groundwater. The isotope composition of deeper soil water horizons and groundwater is constant and close to annual (weighted) mean isotope signature of precipitation (e.g. Herrmann et al., 1987). Therefore, during summer time, when the plants are photosynthetic active, plant source water is in isotope disequilibrium with atmospheric water vapour to which the leaves are exposed. The impact on the calculated RH values of the possible lack of equilibrium between plant source water (having the expected isotope signature equal to that of annual weighted mean of local precipitation) and the local atmospheric water vapour during vegetation period, was evaluated using the data provided by Jacob and Sonntag (1991), who measured isotope composition of precipitation and atmospheric water vapour in Heidelberg, Germany during the period 1981 to 1989. The mean difference between source water to water vapour equilibrium fractionation (= ε*) calculated for the vegetation period (April-October) and the apparent fractionation (ε_{ap}), derived from Jacob and Sonntag (1991) data, amounts to 18.3 and 1.57‰ for ^2H and ^{18}O, respectively (ε_{ap} is smaller than ε*). This apparent fractionation was then used in Eq. (1) instead of the difference δ_a - δ_s and RH values were recalculated. The effect of this replacement, however, lead to an average RH changes of only -1.7% (±0.9), which is far below the analytical errors of the deuterium-excess of leaf water. Apart from a potential disequilibrium between the atmospheric water vapor

Climate
of the Past
Discussions

and the source water, also variable air temperatures can alter the LEL slope. However, a temperature change of ± 10°C shift the reconstructed RH_{dv} values just around ± 1%, via slightly different equilibrium fractionation parameters (leading to an LEL slope range from 3.0 to 2.6; cf. section 2.4). This temperature range largely exceed the expected variation throughout the

5   Late Glacial to Early Holocene transition, inferred e.g. from plant-based mean July temperatures from Isarin and Bohncke (1999). This is in line with the previous finding that such temperature changes are negligible for the relative humidity reconstruction compared to the measurement errors of biomarker isotope analyses (cf. Zech et al., 2013a, and discussion therein). Overall, the used LEL slope of 2.8 (Fig. 4), as well as the above presented range for

10   possibly temperature changes, are well in agreement with field and laboratory studies (Allison et al., 1985; Bariac et al., 1994; Gat et al., 2007; Tipple et al., 2013; Walker and Brunel, 1990).

A further assumption of the presented paleohygrometer approach is that Δd are solely interpreted as the result of leaf water isotope changes and should thus reflect changes in leaf water evaporative enrichment (Hepp et al., 2017; Tuthorn et al., 2015; Zech et al., 2013a).

15   Indeed, the evaporative enrichment of leaf water is strongly driven by the relative air humidity in the direct surrounding of the leaf (e.g. Eq. 3; Cernusak et al., 2016). However, soil water enrichment is not accounted. Generally, soil water enrichment would shift the plant soil water along the soil evaporation line right of the $LWML_{Germany}$, for which our model does not account leading to an underestimation of RH if, in spite of this, the deuterium-excess of the

20   $LMWL_{Germany}$ approximates d_s. Soil water evaporation typically affects only the upper centimeters of the soil (~ 10 cm; Dubbert et al., 2013), while the trees utilize deeper and thus unenriched soil water (Dawson, 1993). An additional prerequisite is the stability of the deuterium-excess and slope of the $LMWL_{Germany}$ through the past. According to Stumpp et al. (2014), the long-term deuterium-excess of precipitation values from 28 sites do not show

25   pronounced relationships to local climate conditions of the site. All reported values are close to 10‰, which indicates that Atlantic air masses are the main moisture source for Germany (e.g. Rozanski et al., 1993). In addition, the deuterium-excess in local precipitation from the close-by stations Trier and Koblenz reveal small variability on monthly, annual and long-term basis compared to the pooled standard error of d_l, which averages at 15‰. For Trier monthly averages

30   (March to October) range from 5.3 to 8.7‰, annual precipitation weighted means from 1.9 to 10.6‰, and long-term precipitation weighted mean is 6.7‰ (±2.2); for Koblenz the values range between 2.1 and 6.4‰, 1.4 and 8.7‰, and the long-term weighted mean is 4.1‰ (±1.8) (derived from IAEA/WMO, 2018). Finally, deuterium-excess variability in Greenland and Antarctic ice-core does not exceed 4‰ over the here relevant time scale (Masson-Delmotte et

al., 2005; Stenni et al., 2010). In addition, paleowater samples from Europe suggest that the atmospheric circulation patterns over European continent were rather constant throughout the past 35,000 years, which also implies that long-term deuterium-excess of precipitation does not deviate substantially from the modern value (Rozanski, 1985). In summary, the variations in

5   the slope of the LMWL of Germany are assumed to be rather small over longer timescales. With regard to the detailed discussion in this section, the RH_{dv} seems to be suitable for paleoclimate record comparison.

3.4 How dry was the Younger Dryas in Western Europe?

10   While it is well known that the Younger Dryas was a cold spell occurring in the Northern Hemisphere during the Late Glacial (Denton et al., 2010; Heiri et al., 2014; Isarin and Bohncke, 1999), there is much less clear evidence concerning moisture supply/availability and relative humidity changes during the Younger Dryas. The Lake Gemündener Maar RH_{dv} results suggest relatively humid conditions at end of the Allerød and the first phase of the Younger Dryas (~

15   56%), which are in the same range as modern RH_{dv} values (Fig. 5B; derived from the adjacent meteorological station Nürburg-Barweiler, approx. 25 km northeast of Lake GM; hourly data from 1995 to 2015 from Deutscher Wetterdienst, 2016). This is followed by a clear RH_{dv} decrease of ~ 11% towards the end of the Younger Dryas, compared to the Allerød and first phase of the Younger Dryas (Fig. 6A). Such a two phasing of the Younger Dryas has been

20   suggested previously based on multiproxy climate data (Isarin et al., 1998). In more detail, Isarin et al. (1998) point to a subdivided Younger Dryas into a cold and humid first phase followed by drier and warmer conditions for western Europe. It is moreover speculated that a shift of the mean sea-ice margin during winter in the North Atlantic Ocean slightly to the north could have caused this two phasing. Reduced cyclonic activity and precipitation affected

25   thereby primarily Western Europe because this region was situated at the southern margin of the main storm tracks during the first Younger Dryas period (Isarin et al., 1998). The authors presented also evidence for a strengthening of the westerly winds in Western Europe as consequence of northwards shifted North Atlantic Ocean sea-ice margin during the late Younger Dryas period. However, the varve thickness record from Lake Meerfelder Maar

30   laminated sediments show a distinctive reduction of the sedimentation rates at 12,240 varve a BP, dividing the Younger Dryas in a first phase with thicker varves while the second period is characterized by slightly reduced sedimentation rate (Brauer et al., 1999). The thicker varves during the early Younger Dryas (between 12,680 and 12,240 varve a BP) are used along with geochemical analysis as indicator for stronger winter winds (Brauer et al., 2008). In line with

Climate
of the Past

Discussions

this, Brauer et al. (1999) interpreted high biogenic opal contents and *Prediastrum* remain concentrations during the early Younger Dryas as enhanced aquatic productivity due to an increased nutrient supply caused by soil erosion and the reworking of littoral sediments. The varve formation throughout the second Younger Dryas period (between 12,240 and 11,590

5   varve a BP) is characterized as mainly controlled by snowmelt driven surface runoff (Brauer et al., 1999). Moreover, the authors speculate if during that time the Meerbach creek came into connection with the Meerfelder Maar, which could be possibly linked to enhanced precipitation amounts. In summary, the interpretations derived from the Younger Dryas sediments of Lake Meefelder Maar (Brauer et al., 2008, 1999) is not in accordance with the results from Isarin et

10   al. (1998), as well as the RH_{dv} results presented here (Fig. 6A). Not fully consistent with both outcomes are the continuously dry conditions during the Younger Dryas, as derived from the difference between terrestrial- and aquatic-plant-derived *n*-alkane δ^2H values extracted from Lake Meefelder Maar sediments (Rach et al., 2014). It should be noted that Rach et al. (2017) used this difference as main input parameter in their dual-biomarker approach. In more detail,

15   the ~ 10% drop of relative humidity changes between the Allerød and the Younger Dryas period is well comparable to the ~ 10% relative humidity difference between the Allerød and the second phase of the Younger Dryas at Lake Gemündener Maar RH_{dv} record (comparisons is based on mean period values). Moreover, the regeneration towards Allerød humidity level around 12,000 a BP, the distinct rise at the end of the Younger Dryas as well as the overall

20   variability obvious in Lake GM reconstructed RH_{dv} values of 50% throughout the Late Glacial to Holocene transition fit well to the relative humidity changes from Lake Meerfelder Maar. Rach et al. (2017) reconstructed a comparable range of ~ 40% throughout the investigated time period covering the Younger Dryas (11,000 to 13,100 varve a BP). However, the continuous dry conditions during the Younger Dryas period reported by Rach et al. (2017, 2014) do not

25   resemble the Lake Gemündener Maar RH_{dv} record. Probably some greater extent of lake water enrichment during the late Allerød and the late Younger Dryas extended the difference between terrestrial and aquatic *n*-alkane δ^2H values, leading consequently to an underestimation of the dryness during those periods. Indeed, Lake Holzmaar, which seems to be comparable to Lake Meefelder Maar at least for the drainage conditions via one creek, shows a difference of 7.4‰

30   in δ^2H between inflow and lake water (Sachse et al., 2004). It is moreover shown by Sachse et al. (2004) that no significant correlation occurs between *n*-C$_{23}$ alkane δ^2H values, between lake water and precipitation along a European lake surface transect. Finally it can be questioned if Lake Meerfelder Maar *n*-C$_{23}$ alkanes solely originate from *Potamogeton* (Rach et al., 2014) with recent publications indicating that *n*-C$_{23}$ is not necessarily interpreted of aquatic origin

35   (Aichner et al., 2018; Rao et al., 2014). Probably some extend could also originate from soil

microbes, transported into the lake sediments during the early Younger Dryas due to high erosion rates (Brauer et al., 1999). In summary, this adds uncertainty to the continuous dryness of the Younger Dryas based on the difference between terrestrial and aquatic n-alkane $\delta^2 H$ values (Rach et al., 2014, 2017). Similarly, these uncertainties could potentially affect the

5   difference between terrestrial and aquatic n-alkane $\delta^2 H$ values from Hässeldala Port Younger Dryas lake sediments from Southern Sweden (Muschitiello et al., 2015). The authors used the approach presented by Rach et al. (2014) with $\delta^2 H$ values of n-C_{21} representative for lake water, respectively summer precipitation, and n-C_{27}, n-C_{29} and n-C_{31} as reflecting leaf water enrichment. The calculated difference between terrestrial and aquatic n-alkane $\delta^2 H$ values

10   suggest more humid conditions at the beginning of the Younger Dryas followed by a more or less steadily trend towards drier conditions, peaking around 11,700 a BP (Muschitiello et al., 2015). This would be, however, in line with Lake Gemündener Maar RH_{dv} minimum between ~ 11,700 and 11,900 a BP, within age uncertainties of the Lake Gemündener Maar age-depth model. A recent publication from the Southern Pyrenees, analyzing triple oxygen and hydrogen

15   isotopes of gypsum to reconstruct relative humidity changes, also report more humid conditions at the beginning of the Younger Dryas compared to middle and the end of this phase (Gázquez et al., 2018).

(Fig. 6)

When searching for a possible driver of relative humidity changes during the Late

20   Glacial to Early Holocene transition, the Lake Gemündener Maar RH_{dv} record can be compared to the ^{14}C production and ^{10}Be flux rates (Fig. 6B), derived from IntCal13 and the Greenland ice-cores (GRIP, GISP2), respectively (Muscheler et al., 2014). Such records are commonly known as solar activity (and thus insolation) proxies (Stuiver and Braziunas, 1988; Vonmoos et al., 2006). Our results suggest that the end of the Allerød and the first phase of the Younger

25   Dryas are characterized by relatively high RH_{dv} and strong centennial-scale variability (Fig. 6A). This coincides with high and strongly variable ^{14}C production and ^{10}Be flux rates. The clear drop of the RH_{dv} values towards the end of the Younger Dryas is also in agreement with a change to a higher solar activity level. Although RH_{dv} initially recovered slightly at the onset of the Holocene, the Preboreal is mostly a phase of low RH_{dv}. Much higher variability is

30   pronounced than throughout the Younger Dryas. Lowest values are recorded during the late Preboreal (~ 10,600 a BP), which coincide with increased solar activity. However, a short (~300 a) and pronounced phase of very high RH_{dv} occurred ~ 11,200 a BP. We dub this wet period the Preboreal Humid Phase, which is again accompanied by low solar activity (Fig. 6A and B). The Preboreal Humid Phase should not be confused with the Preboreal Oscillation (Björck et

Climate
of the Past
Discussions

al., 1997). The Preboreal Oscillation is a short cold event recorded in Greenland ice-cores ~11,400 ka (Rasmussen et al., 2007) and led to more arid conditions at least in the Netherlands according to palynological results (Bos et al., 2007; van der Plicht et al., 2004). These pollen records also show the existence of a pronounced humid phase thereafter, i.e. the Preboreal

5   Humid Phase. Widespread glacial advances in the Alps are also attributed to the Preboreal Oscillation (Moran et al., 2016), but given the dating uncertainties they may actually rather reflect increased precipitation during the Preboreal Humid Phase. Lake Gemündener Maar RH_{dv} record is overall in good agreement with other local and regional paleoclimate reconstructions. The coherence between RH_{dv} and solar activity, in particular during the

10 Younger Dryas and Preboreal Humid Phase, suggests a possible causality. It is widely accepted that the Younger Dryas and the Preboreal Oscillation are related to freshwater forcing in the North Atlantic (e.g. Fisher et al., 2002; Murton et al., 2010; Muschitiello et al., 2015). However, the causes and mechanisms responsible for climate and environmental changes during the rest of Holocene remain vague, and more research is needed to investigate the possible influence of

15 solar activity (Renssen et al., 2007; Rind, 2002). This can also be inferred from the conducted Monte-Carlo-Simulation based correlation procedure between Lake Gemündener Maar RH_{dv} values and the IntCal13 ^{14}C production rates, which gives a maximum correlation coefficient of 0.37. As such, ~ 14% variability in the Lake Gemündener Maar RH_{dv} record can be explained by solar activity changes. This is achieved when the ^{14}C charcoal age, the onset of the Holocene

20 and the onset of *Corylus* pollen were set to 13,716, 11,557 and 10,675 a BP, respectively. However, in terms of deviation to the non-adjusted dates these are changes of +84, +93 and -225 a. The adjustment of the onset of the *Corylus* pollen in Lake Gemündener Maar was therefore set to the maximum oldest age suggesting that for a more detailed driver analysis individual dated climate archives are urgently needed and that the results presented here should

25 not be over interpreted. Apart from these age-depth model uncertainties of the GM, we argue a conceivably driving mechanism for the RH_{dv} variability in Central Europe could be a combination of solar activity changes, which triggered solar insolation, and North Atlantic Ocean temperature evolution. A key example might be the Preboreal Humid Phase. It can be expected that the North Atlantic Ocean, the main moisture source for Central Europe, revealed

30 already considerable higher temperatures during the Preboreal Humid Phase compared to the Younger Dryas, as indicated by a consistent ~ 2°C increase in planktonic foraminifera (*Globorotalia inflata*, *Globorotalia bulloides* and *Neogloboquadrina pachyderma*) derived Mg/Ca temperatures from a marine sediment core south of Iceland (Thornalley et al., 2009, 2010, 2011). In summary, this could lead to an enhanced moisture content of the atmosphere.

35 When these wetter air masses were transported on continental Europe, where low solar

Climate
of the Past

Discussions

Open Access

EGU

insolation inhibited warming up and drying of these air masses, more humid climate conditions were established. Yet, it can be only speculated if the solar activity minimum during the early Younger Dryas (Fig. 6B) together with strong winds (Brauer et al., 2008) established climatic boundary conditions favoring sea water evaporation, which might have led to increased RH_{dv}

5   in Western Europe (Fig. 6A). Moreover, during the second phase of the Younger Dryas, in which a slight cooling of the North Atlantic Ocean coinciding with increasing solar activity, the climatic conditions on the European continent could have become drier, as suggested by the Lake Gemündener Maar RH_{dv} record. In this light, the applied $\delta^2H_{n\text{-alkane}}$-$\delta^{18}O_{sugar}$ approach has great potential for establishing more quantitative relative humidity records, offering a

10   paleohygrometer approach for better understanding of past climate change.

4 Conclusions

Referring to the underlying research questions and based on the presented results and the outlined discussion (including the cited literature) the following conclusions have to be

15   drawn:

- The terrestrial vs. aquatic origin of bulk sedimentary organic matter cannot be determined unambiguously for the Gemündener Maar. This is caused by the bulk proxies (TOC/TN, $\delta^{13}C$ and $\delta^{15}N$) being not straightforward interpretable. At the same time, this also hampers inferring paleoclimate information based on those proxies. By

20   contrast, the alkane biomarkers with the chain-length n-C_{27} and n-C_{29} and the sugar biomarker arabinose can be most likely associated with the epicuticular leaf-wax layer and the hemicellulose structures of higher terrestrial plants, respectively. Therefore, they are assumed to originate primarily from leaf material of the Gemündener Maar catchment, which enabled us to use them in the coupled δ^2H-$\delta^{18}O$ paleohygrometer

25   approach.

- Leaf water can be accessed from $\delta^2H_{n\text{-alkane}}$ (n-C_{27} and n-C_{29}) and $\delta^{18}O_{sugar}$ (arabinose) by applying constant biosynthetic fractionation factors. We acknowledge that the assumption of constant fractionation factors introduces considerable uncertainties as highlighted by the broad literature discussion. Additionally, a correction for the

30   reconstructed leaf water isotope composition seems to be required to account for grassy n-alkane (n-C_{27} and n-C_{29}) and arabinose contribution, because grasses are known to be less sensitive leaf water enrichment recorders.

- The reconstruction of relative humidity values is quite robust; it does not depend strongly on different scenarios used for calculating leaf water values. Furthermore, a correction to account for possible differences between Craig-Gordon modeled and measured leaf water isotope composition turned out to be dispensable for the here applied paleohyrometer approach. A constant leaf water evaporation line throughout the past seems to be a valid assumption. This was shown by alternative relative air humidity calculations based on apparent fractionation values, which account for a possible lack of equilibrium between plant source water and local atmospheric water vapour. The differences to the conventional reconstructed relative air humidity values (via Eq. 5) are far below the analytical errors associated with $\delta^2 H_{n\text{-alkane}}$ and $\delta^{18} O_{sugar}$ measurements. Moreover, the used local meteoric water line of Germany seems to be a solid base line here. The reconstructed relative air humidity values are interpreted to reflect RH of the vegetation period and the daytime (RH_{dv}).

- The established Lake Gemündener Maar RH_{dv} record supports a two-phasing of the Younger Dryas, i.e. a relative wet phase on Allerød level followed by a drier Younger Dryas ending. Overall drier climatic conditions throughout the Younger Dryas or a two-phasing in terms of a first dry and cold Younger Dryas phase followed by a warmer period along with increasing precipitation amounts could not be corroborated. Surprisingly, the amplitude of RH_{dv} changes during the Early Holocene was more pronounced compared to the Younger Dryas. One possible driver for the unexpected Lake Gemündener Maar RH_{dv} variations could be the solar activity, as derived from the comparison with IntCal ^{14}C production and Greenland ice-core [10]Be flux rate data.

Data availability

The data will be made available upon request.

Author contributions

**Climate
of the Past**
Discussions

Open Access

EGU

References

Aichner, B., Ott, F., Słowiński, M., Noryśkiewicz, A. M., Brauer, A. and Sachse, D.: Leaf wax *n*-alkane
distributions record ecological changes during the Younger Dryas at Trzechowskie paleolake (Northern
20   Poland) without temporal delay, Climate of the Past Discussions, (March), 1–29, doi:10.5194/cp-2018-6,
2018.
Alley, R. B.: The Younger Dryas cold interval as viewed from central Greenland, Quaternary Science Reviews,
19(1–5), 213–226, doi:10.1016/S0277-3791(99)00062-1, 2000.
Allison, G. B., Gat, J. R. and Leaney, F. W. J.: The relationship between deuterium and oxygen-18 delta values
25   in leaf water, Chemical Geology, 58, 145–156, 1985.
Altabet, M. A., Francois, R., Murray, D. W. and Prell, W. L.: Climate-related variations in denitrification in the
Arabian Sea from sediment ^{15}N/^{14}N ratios, Nature, 373, 506–509, 1995.
Altermatt, H. A. and Neish, A. C.: The biosynthesis of cell wall carbohydrates: III. Further studies on formation
of cellulose and xylan from labeled monosaccharides in wheat plants, Canadian Journal of Biochemistry
30   and Physiology, 34(3), 405–413, doi:10.1139/o56-042, 1956.
Amelung, W., Cheshire, M. V. and Guggenberger, G.: Determination of neutral and acidic sugars in soil by
capillary gas-liquid chromatography after trifluoroacetic acid hydrolysis, Soil Biology and Biochemistry,
28(12), 1631–1639, 1996.
Araguás-Araguás, L., Froehlich, K. and Rozanski, K.: Deuterium and oxygen-18 isotope composition of
35   precipitation and atmospheric moisture, Hydrological Processes, 14(8), 1341–1355, doi:10.1002/1099-
1085(20000615)14:8<1341::AID-HYP983>3.0.CO;2-Z, 2000.
Barbour, M. M.: Stable oxygen isotope composition of plant tissue: a review, Functional Plant Biology, 34, 83–
94, doi:http://dx.doi.org/10.1071/FP06228, 2007.
Barbour, M. M. and Farquhar, G. D.: Relative humidity-and ABA-induced variation in carbon and oxygen
40   isotope ratios of cotton leaves, Plant, Cell & Environment, 23(5), 473–485, 2000.
Barbour, M. M., Roden, J. S., Farquhar, G. D. and Ehleringer, J. R.: Expressing leaf water and cellulose oxygen
isotope ratios as enrichment above source water reveals evidence of a Péclet effect, Oecologia, 138(3),
426–435, doi:10.1007/s00442-003-1449-3, 2004.
Bariac, T., Gonzalez-Dunia, J., Katerji, N., Béthenod, O., Bertolini, J. M. and Mariotti, A.: Spatial variation of
45   the isotopic composition of water (^{18}O, ^{2}H) in the soil-plant-atmosphere system, 2. Assessment under field

conditions, Chemical Geology, 115, 317–333, 1994.

Björck, S., Rundgren, M., Ingólfsson, O. and Funder, S.: The Preboreal oscillation around the Nordic Seas: terrestrial and lacustrine responses, Journal of Quaternary Science, 12(6), 455–465, doi:10.1002/(SICI)1099-1417(199711/12)12, 1997.

5   Bos, J. A. A., van Geel, B., van der Plicht, J. and Bohncke, S. J. P.: Preboreal climate oscillations in Europe: Wiggle-match dating and synthesis of Dutch high-resolution multi-proxy records, Quaternary Science Reviews, 26(15–16), 1927–1950, doi:10.1016/j.quascirev.2006.09.012, 2007.

Brauer, A., Endres, C., Günter, C., Litt, T., Stebich, M. and Negendank, J. F. W.: High resolution sediment and vegetation responses to Younger Dryas climate change in varved lake sediments from Meerfelder Maar,
10   Germany, Quaternary Science Reviews, 18(3), 321–329, doi:10.1016/S0277-3791(98)00084-5, 1999.

Brauer, A., Haug, G. H., Dulski, P., Sigman, D. M. and Negendank, J. F. W.: An abrupt wind shift in western Europe at the onset of the Younger Dryas cold period, Nature Geoscience, 1(8), 520–523, doi:10.1038/ngeo263, 2008.

Brunck, H., Sirocko, F. and Albert, J.: The ELSA-Flood-Stack: A reconstruction from the laminated sediments
15   of Eifel maar structures during the last 60,000 years, Global and Planetary Change, 142, 136–146, doi:10.1016/j.gloplacha.2015.12.003, 2015.

Büchel, G.: Maars of the Westeifel, Germany, in Paleolimnology of European Maar Lake, vol. 49, edited by L. Negendank and B. Zolitschka, pp. 1–13, Springer-Verlag, Berlin Heidelberg., 1993.

Büchel, G.: Vulkanologische Karte der West- und Hocheifel 1:50000, Koblenz., 1994.

20   Burget, E. G., Verma, R., Mølhøj, M. and Reiter, W.-D.: The Biosynthesis of L-Arabinose in Plants: Molecular Cloning and Characterization of a Golgi-Localized UDP-D-Xylose 4-Epimerase Encoded by the MUR4 Gene of Arabidopsis, Plant Cell, 15(February), 523–531, doi:10.1105/tpc.008425.response, 2003.

Cernusak, L. A., Wong, S. C. and Farquhar, G. D.: Oxygen isotope composition of phloem sap in relation to leaf water in Ricinus communis, Functional Plant Biology, 30(10), 1059–1070, 2003.

25   Cernusak, L. A., Farquhar, G. D. and Pate, J. S.: Environmental and physiological controls over oxygen and carbon isotope composition of Tasmanian blue gum, *Eucalyptus globulus*, Tree Physiology, 25(2), 129–146, doi:10.1093/treephys/25.2.129, 2005.

Cernusak, L. A., Barbour, M. M., Arndt, S. K., Cheesman, A. W., English, N. B., Feild, T. S., Helliker, B. R., Holloway-Phillips, M. M., Holtum, J. A. M., Kahmen, A., Mcinerney, F. A., Munksgaard, N. C., Simonin,
30   K. A., Song, X., Stuart-Williams, H., West, J. B. and Farquhar, G. D.: Stable isotopes in leaf water of terrestrial plants, Plant Cell and Environment, 39(5), 1087–1102, doi:10.1111/pce.12703, 2016.

Cheesman, A. W. and Cernusak, L. A.: Infidelity in the outback: Climate signal recorded in $\Delta^{18}O$ of leaf but not branch cellulose of eucalypts across an Australian aridity gradient, Tree Physiology, 37(5), 554–564, doi:10.1093/treephys/tpw121, 2017.

35   Craig, H. and Gordon, L. I.: Deuterium and oxygen-18 variations in the ocean and the marine atmosphere, in Proceedings of a Conference on Stable Isotopes in Oceanographic Studies and Palaeotemperatures, edited by E. Tongiorgi, pp. 9–130, Lischi and Figli, Pisa., 1965.

Dansgaard, W.: Stable isotopes in precipitation, Tellus, 16(4), 436–468, doi:10.1111/j.2153-3490.1964.tb00181.x, 1964.

40   Dawson, T. E.: Hydraulic lift and water use by plants: implications for water balance, performance and plant-plant interactions, Oecologia, 95(4), 565–574, 1993.

Denton, G. H., Anderson, R. F., Toggweiler, J. R., Edwards, R. L., Schaefer, J. M. and Putnam, A. E.: The Last Glacial Termination, Science, 328(5986), 1652–1656, doi:10.1126/science.1184119, 2010.

Deutscher Wetterdienst: Climate data center, Nürburg-Barweiler station [online] Available from: ftp://ftp-
45   cdc.dwd.de/pub/CDC/ (Accessed 10 August 2016), 2016.

Dubbert, M., Cuntz, M., Piayda, A., Maguás, C. and Werner, C.: Partitioning evapotranspiration - Testing the Craig and Gordon model with field measurements of oxygen isotope ratios of evaporative fluxes, Journal of Hydrology, 496, 142–153, doi:10.1016/j.jhydrol.2013.05.033, 2013.

Eglinton, G. and Hamilton, R. J.: Leaf Epicuticular Waxes, Science, 156(3780), 1322–1335,
50   doi:10.1126/science.156.3780.1322, 1967.

Farquhar, G. D., Hubick, K. T., Condon, A. G. and Richards, R. A.: Carbon Isotope Fractionation and Plant Water-Use Efficiency, in Stable Isotopes in Ecological Research. Ecological Studies (Analysis and Synthesis), vol. 68, edited by P. W. Rundel, J. R. Ehleringer, and K. A. Nagy, pp. 21–40, Springer-Verlag, New York., 1989.

55   Feng, X., Reddington, A. L., Faiia, A. M., Posmentier, E. S., Shu, Y. and Xu, X.: The changes in North American atmospheric circulation patterns indicated by wood cellulose, Geology, 35(2), 163–166, doi:10.1130/G22884A.1, 2007.

Fisher, T. G., Smith, D. G. and Andrews, J. T.: Preboreal oscillation caused by a glacial Lake Agassiz flood, Quaternary Science Reviews, 21(8–9), 873–878, doi:10.1016/S0277-3791(01)00148-2, 2002.

60   Flanagan, L. B., Comstock, J. P. and Ehleringer, J. R.: Comparison of Modeled and Observed Environmental Influences on the Stable Oxygen and Hydrogen Isotope Composition of Leaf Water in Phaseolus vulgaris L., Plant Physiology, (96), 588–596, 1991.

Gamarra, B., Sachse, D. and Kahmen, A.: Effects of leaf water evaporative [2]H-enrichment and biosynthetic
   fractionation on leaf wax *n*-alkane δ^{2}H values in C3 and C4 grasses, Plant, Cell and Environment
   Environment, 39, 2390–2403, doi:10.1111/pce.12789, 2016.

5   Gat, J. R. and Bowser, C. J.: The heavy isotope enrichment of water in coupled evaporative systems, in Stable
   Isotope Geochemistry: A Tribute to Samuel Epstein, vol. 3, edited by H. P. Tayler, J. R. O'Neil, and I. R.
   Kaplan, pp. 159–168, The Geochemical Society, Lancester., 1991.

Gat, J. R., Yakir, D., Goodfriend, G., Fritz, P., Trimborn, P., Lipp, J., Gev, I., Adar, E. and Waisel, Y.: Stable
   isotope composition of water in desert plants, Plant and Soil, 298(1--2), 31–45, doi:10.1007/s11104-007-
   9321-6, 2007.

10 Gázquez, F., Morellón, M., Bauska, T., Herwartz, D., Surma, J., Moreno, A., Staubwasser, M., Valero-Garcés,
   B., Delgado-Huertas, A. and Hodell, D. A.: Triple oxygen and hydrogen isotopes of gypsum hydration
   water for quantitative paleo-humidity reconstruction, Earth and Planetary Science Letters, 481, 177–188,
   doi:10.1016/j.epsl.2017.10.020, 2018.

Gross, S. and Glaser, B.: Minimization of carbon addition during derivatization of monosaccharides for
15   compound-specific δ^{13}C analysis in environmental research, Rapid Communications in Mass Spectrometry,
   18, 2753–2764, doi:10.1002/rcm.1684, 2004.

Harper, A. D. and Bar-Peled, M.: Biosynthesis of UDP-Xylose. Cloning and Characterization of a Novel
   Arabidopsis Gene Family, UXS, Encoding Soluble and Putative Membrane-Bound UDP-Glucuronic Acid
   Decarboxylase Isoforms, Gene, 130(December), 2188–2198, doi:10.1104/pp.009654.2188, 2002.

20 Harris, D., Horwáth, W. R. and van Kessel, C.: Acid fumigation of soils to remove carbonates prior to total
   organic carbon or carbon-13 isotopic analysis, Soil Science Society of America Journal, 65(6), 1853,
   doi:10.2136/sssaj2001.1853, 2001.

Heiri, O., Koinig, K. A., Spötl, C., Barrett, S., Brauer, A., Drescher-Schneider, R., Gaar, D., Ivy-Ochs, S.,
   Kerschner, H., Luetscher, M., Moran, A., Nicolussi, K., Preusser, F., Schmidt, R., Schoeneich, P.,
25   Schwörer, C., Sprafke, T., Terhorst, B. and Tinner, W.: Palaeoclimate records 60-8 ka in the Austrian and
   Swiss Alps and their forelands, Quaternary Science Reviews, 106(December), 186–205,
   doi:10.1016/j.quascirev.2014.05.021, 2014.

Helliker, B. R. and Ehleringer, J. R.: Grass blades as tree rings: environmentally induced changes in the oxygen
   isotope ratio of cellulose along the length of grass blades, New Phytologist, 155, 417–424, 2002.

30 Henderson, A. K., Nelson, D. M., Hu, F. S., Huang, Y., Shuman, B. N. and Williams, J. W.: Holocene
   precipitation seasonality captured by a dual hydrogen and oxygen isotope approach at Steel Lake,
   Minnesota, Earth and Planetary Science Letters, 300(3--4), 205–214,
   doi:http://dx.doi.org/10.1016/j.epsl.2010.09.024, 2010.

Hepp, J., Tuthorn, M., Zech, R., Mügler, I., Schlütz, F., Zech, W. and Zech, M.: Reconstructing lake evaporation
35   history and the isotopic composition of precipitation by a coupled δ^{18}O–δ^{2}H biomarker approach, Journal of
   Hydrology, 529, 622–631, 2015.

Hepp, J., Rabus, M., Anhäuser, T., Bromm, T., Laforsch, C., Sirocko, F., Glaser, B. and Zech, M.: A sugar
   biomarker proxy for assessing terrestrial versus aquatic sedimentary input, Organic Geochemistry, 98, 98–
   104, doi:10.1016/j.orggeochem.2016.05.012, 2016.

40 Hepp, J., Zech, R., Rozanski, K., Tuthorn, M., Glaser, B., Greule, M., Keppler, F., Huang, Y., Zech, W. and
   Zech, M.: Late Quaternary relative humidity changes from Mt. Kilimanjaro, based on a coupled [2]H-[18]O
   biomarker paleohygrometer approach, Quaternary International, 438, 116–130,
   doi:10.1016/j.quaint.2017.03.059, 2017.

Hepp, J., Schäfer, I., Tuthorn, M., Glaser, B., Juchelka, D., Rozanski, K., Stichler, W., Zech, R., Mayr, C. and
45   Zech, M.: Validiation of acoupled δ^{2}H$_{n-alkane}$-δ^{18}O$_{sugar}$ paleohygrometer approach based on a climate
   chamber experiment, submitted to GCA, 2018.

Herrmann, A., Maloszewski, P. and Stichler, W.: Changes of [18]O contents of precipitation water during seepage
   in the unsaturated zone, in Proceedings of International Symposium on Groundwater Monitoring and
   Management, 23 - 28 March, p. 22, Institut of Water Management Berlin (GDR) with support of UNESCO,
50   Dresden., 1987.

Horita, J. and Wesolowski, D. J.: Liquid-vapor fractionation of oxygen and hydrogen isotopes of water from the
   freezing to the critical temperature, Geochimica et Cosmochimica Acta, 58(16), 3425–3437,
   doi:http://dx.doi.org/10.1016/0016-7037(94)90096-5, 1994.

Hou, J., D'Andrea, W. J. and Huang, Y.: Can sedimentary leaf waxes record D/H ratios of continental
55   precipitation? Field, model, and experimental assessments, Geochimica et Cosmochimica Acta, 72, 3503–
   3517, doi:10.1016/j.gca.2008.04.030, 2008.

Huang, Y., Shuman, B., Wang, Y. and Iii, T. W.: Hydrogen isotope ratios of individual lipids in lake sediments
   as novel tracers of climatic and environmental change: a surface sediment test, Journal of Paleolimnology,
   31, 363–375, 2004.

60 IAEA/WMO: Global Network of Isotopes in Precipitation. The GNIP Database, [online] Available from:
   https://nucleus.iaea.org/wiser (Accessed 9 February 2018), 2018.

Isarin, R. F. B. and Bohncke, S. J. P.: Mean July Temperatures during the Younger Dryas in Northwestern and

**Climate
of the Past
Discussions**

Central Europe as Inferred from Climate Indicator Plant Species, Quaternary Research, 51(02), 158–173, doi:10.1006/qres.1998.2023, 1999.

Isarin, R. F. B., Renssen, H. and Vandenberghe, J.: The impact of the North Atlantic Ocean on the Younger Dryas climate in northwestern and central Europe, Journal of Quaternary Science, 13(5), 447–453, doi:10.1002/(sici)1099-1417(1998090)13:5<447::aid-jqs402>3.0.co;2-b, 1998.

Jacob, H. and Sonntag, C.: An 8-year record of the seasonal- variation of ^{2}H and ^{18}O in atmospheric water vapor and precipitation at Heidelberg, Tellus, 43B(3), 291–300, 1991.

Jia, G., Dungait, J. A. J., Bingham, E. M., Valiranta, M., Korhola, A. and Evershed, R. P.: Neutral monosaccharides as biomarker proxies for bog-forming plants for application to palaeovegetation reconstruction in ombrotrophic peat deposits, Organic Geochemistry, 39(12), 1790–1799, doi:10.1016/j.orggeochem.2008.07.002, 2008.

Kahmen, A., Sachse, D., Arndt, S. K., Tu, K. P., Farrington, H., Vitousek, P. M. and Dawson, T. E.: Cellulose δ^{18}O is an index of leaf-to-air vapor pressure difference (VPD) in tropical plants, Proceedings of the National Academy of Sciences of the United States of America, 108(5), 1981–1986, doi:10.1073/pnas.1018906108, 2011a.

Kahmen, A., Dawson, T. E., Vieth, A. and Sachse, D.: Leaf wax *n*-alkane δD values are determined early in the ontogeny of Populus trichocarpa leaves when grown under controlled environmental conditions, Plant, Cell and Environment, 34(10), 1639–1651, doi:10.1111/j.1365-3040.2011.02360.x, 2011b.

Kahmen, A., Schefuß, E. and Sachse, D.: Leaf water deuterium enrichment shapes leaf wax *n*-alkane δD values of angiosperm plants I: Experimental evidence and mechanistic insights, Geochimica et Cosmochimica Acta, 111, 39–49, 2013a.

Kahmen, A., Hoffmann, B., Schefuß, E., Arndt, S. K., Cernusak, L. A., West, J. B. and Sachse, D.: Leaf water deuterium enrichment shapes leaf wax *n*-alkane δD values of angiosperm plants II: Observational evidence and global implications, Geochimica et Cosmochimica Acta, 111, 50–63, doi:10.1016/j.gca.2012.09.004, 2013b.

Knapp, D. R.: Handbook of Analytical Derivatization Reactions, John Wiley & Sons, New York, Chichester, Brisbane, Toronto, Singapore., 1979.

Lehmann, M. M., Gamarra, B., Kahmen, A., Siegwolf, R. T. W. and Saurer, M.: Oxygen isotope fractionations across individual leaf carbohydrates in grass and tree species, Plant Cell and Environment, 40(8), 1658–1670, doi:10.1111/pce.12974, 2017.

Litt, T. and Stebich, M.: Bio- and chronostratigraphy of the lateglacial in the Eifel region, Germany, Quaternary International, 61(1999), 5–16, doi:10.1016/S1040-6182(99)00013-0, 1999.

Litt, T., Brauer, A., Goslar, T., Merkt, J., Balaga, K., Müller, H., Ralska-Jasiewiczowa, M., Stebich, M. and Negendank, J. F. W.: Correlation and synchronisation of Lateglacial continental sequences in northern central Europe based on annually laminated lacustrine sediments, Quaternary Science Reviews, 20, 1233,1249, 2001.

Litt, T., Schmincke, H.-U. and Kromer, B.: Environmental response to climatic and volcanic events in central Europe during the Weichselian Lateglacial, Quaternary Science Reviews, 22, 7–32, 2003.

Liu, H. T., Gong, X. Y., Schäufele, R., Yang, F., Hirl, R. T., Schmidt, A. and Schnyder, H.: Nitrogen fertilization and δ^{18}O of CO$_2$ have no effect on ^{18}O-enrichment of leaf water and cellulose in *Cleistogenes squarrosa* (C$_4$) – is VPD the sole control?, Plant Cell and Environment, 39(12), 2701–2712, doi:10.1111/pce.12824, 2016.

Liu, H. T., Schäufele, R., Gong, X. Y. and Schnyder, H.: The δ^{18}O and δ^{2}H of water in the leaf growth-and-differentiation zone of grasses is close to source water in both humid and dry atmospheres, New Phytologist, 214(4), 1423–1431, doi:10.1111/nph.14549, 2017.

Lücke, A., Schleser, G. H., Zolitschka, B. and Negendank, J. F. W.: A Lateglacial and Holocene organic carbon isotope record of lacustrine palaeoproductivity and climatic change derived from varved lake sediments of Lake Holzmaar, Germany, Quaternary Science Reviews, 22(5–7), 569–580, doi:10.1016/S0277-3791(02)00187-7, 2003.

Luetscher, M., Boch, R., Sodemann, H., Spötl, C., Cheng, H., Edwards, R. L., Frisia, S., Hof, F. and Müller, W.: North Atlantic storm track changes during the Last Glacial Maximum recorded by Alpine speleothems, Nature Communications, 6, 6344, doi:10.1038/ncomms7344, 2015.

Masson-Delmotte, V., Jouzel, J., Landais, A., Stievenard, M., Johnson, S. J., White, J. W. C., Werner, M., Sveinbjornsdottir, A. and Fuhrer, K.: GRIP Deuterium Excess Reveals Rapid and Orbital-Scale Changes in Greenland Moisture Origin, Science, 309, 118–121, doi:10.1126/science.1108575, 2005.

Merlivat, L.: Molecular diffusivities of H$_2$^{16}O, HD^{16}O, and H$_2$^{18}O in gases, The Journal of Chemical Physics, 69(6), 2864–2871, doi:http://dx.doi.org/10.1063/1.436884, 1978.

Meyers, P. A. and Ishiwatari, R.: Lacustrine organic geochemistry - an overview of indicators of organic matter sources and diagenesis in lake sediments, Organic Geochemistry, 20(7), 867–900, 1993.

Meyers, P. A. and Lallier-Vergés, E.: Lacustrine Sedimentary Organic Matter Records of Late Quaternary Paleoclimates, Journal of Paleolimnology, 21(3), 345–372, doi:10.1023/A:1008073732192, 1999.

Moran, A. P., Ivy-Ochs, S., Vockenhuber, C. and Kerschner, H.: First ^{36}Cl exposure ages from a moraine in the

Climate
of the Past

Discussions

Northern Calcareous Alps, Eiszeitalter und Gegenwart – Quaternary Science Journal, 65(2), 145–155, doi:10.3285/eg.65.2.03, 2016.

Mügler, I., Sachse, D., Werner, M., Xu, B., Wu, G., Yao, T. and Gleixner, G.: Effect of lake evaporation on δD values of lacustrine *n*-alkanes: A comparison of Nam Co (Tibetan Plateau) and Holzmaar (Germany), Organic Geochemistry, 39(6), 711–729, 2008.

Murton, J. B., Bateman, M. D., Dallimore, S. R., Teller, J. T. and Yang, Z.: Identification of Younger Dryas outburst flood path from Lake Agassiz to the Arctic Ocean, Nature, 464(7289), 740–743, doi:10.1038/nature08954, 2010.

Muscheler, R., Adolphi, F. and Knudsen, M. F.: Assessing the differences between the IntCal and Greenland ice-core time scales for the last 14,000 years via the common cosmogenic radionuclide variations, Quaternary Science Reviews, 106, 81–87, doi:10.1016/j.quascirev.2014.08.017, 2014.

Muschitiello, F., Pausata, F. S. R., Watson, J. E., Smittenberg, R. H., Salih, A. A. M., Brooks, S. J., Whitehouse, N. J., Karlatou-Charalampopoulou, A. and Wohlfarth, B.: Fennoscandian freshwater control on Greenland hydroclimate shifts at the onset of the Younger Dryas, Nature Communications, 6, 8939, doi:10.1038/ncomms9939, 2015.

Natelhoffer, K. J. and Fry, B.: Controls on Natural Nitrogen-15 and Carbon-13 Abundances in Forest Soil Organic Matter, Soil Science Society of America Journal, 52(6), 1633–1640, doi:doi:10.2136/sssaj1988.03615995005200060024x, 1988.

Parker, G. G.: Structure and Mircoclimate of Canopies, in Forest Canopies, edited by M. D. Lowman and N. M. Nadkarni, pp. 73–106, Academic Press, San Diego., 1995.

Partin, J. W., Quinn, T. M., Shen, C.-C., Okumura, Y., Cardenas, M. B., Siringan, F. P., Banner, J. L., Lin, K., Hu, H.-M. and Taylor, F. W.: Gradual onset and recovery of the Younger Dryas abrupt climate event in the tropics, Nature Communications, 6, 8061, doi:10.1038/ncomms9061, 2015.

Peterson, B. J., Howarth, R. W. and Garritt, R. H.: Multiple Stable Isotopes Used to Trace the Flow of Organic Matter in Estuarine Food Webs, Science, 227(4692), 1361–1363, doi:10.1126/science.227.4692.1361, 1985.

van der Plicht, J., van Geel, B., Bohncke, S. J. P., Bos, J. A. A., Blaauw, M., Speranza, A. O. M., Muscheler, R. and Björck, S.: The Preboreal climate reversal and a subsequent solar-forced climate shift, Journal of Quaternary Science, 19(3), 263–269, doi:10.1002/jqs.835, 2004.

Prahl, F. G., Bennett, J. T. and Carpenter, R.: The early diagenesis of aliphatic hydrocarbons and organic matter in sedimentary particulates from Dabob Bay, Washington, Geochimica et Cosmochimica Acta, 44(12), 1967–1976, doi:10.1016/0016-7037(80)90196-9, 1980.

Prietzel, J., Dechamps, N. and Spielvogel, S.: Analysis of non-cellulosic polysaccharides helps to reveal the history of thick organic surface layers on calcareous Alpine soils, Plant and Soil, 365(1–2), 93–114, doi:10.1007/s11104-012-1340-2, 2013.

R Core Team: R: A Language and Environment for Statistical Computing, [online] Available from: https://www.r-project.org/, 2015.

Rach, O., Brauer, A., Wilkes, H. and Sachse, D.: Delayed hydrological response to Greenland cooling at the onset of the Younger Dryas in western Europe, Nature Geoscience, 7(1), 109–112, doi:10.1038/ngeo2053, 2014.

Rach, O., Kahmen, A., Brauer, A. and Sachse, D.: A dual-biomarker approach for quantification of changes in relative humidity from sedimentary lipid D/H ratios, Climate of the Past, 13, 741–757, doi:10.5194/cp-2017-7, 2017.

Rao, Z., Zhu, Z., Jia, G., Henderson, A. C. G., Xue, Q. and Wang, S.: Compound specific δD values of long chain *n*-alkanes derived from terrestrial higher plants are indicative of the δD of meteoric waters: Evidence from surface soils in eastern China, Organic Geochemistry, 40(8), 922–930, doi:http://dx.doi.org/10.1016/j.orggeochem.2009.04.011, 2009.

Rao, Z., Jia, G., Qiang, M. and Zhao, Y.: Assessment of the difference between mid- and long chain compound specific δD$_{n\text{-alkanes}}$ values in lacustrine sediments as a paleoclimatic indicator, Organic Geochemistry, 76, 104–117, doi:10.1016/j.orggeochem.2014.07.015, 2014.

Rasmussen, S. O., Andersen, K. K., Svensson, A. M., Steffensen, J. P., Vinther, B. M., Clausen, H. B., Siggaard-Andersen, M.-L., Johnsen, S. J., Larsen, L. B., Dahl-Jensen, D., Bigler, M., Röthlisberger, R., Fischer, H., Goto-Azuma, K., Hansson, M. E. and Ruth, U.: A new Greenland ice core chronology for the last glacial termination, Journal of Geophysical Research: Atmospheres, 111(D6), 1–16, doi:10.1029/2005JD006079, 2006.

Rasmussen, S. O., Vinther, B. M., Clausen, H. B. and Andersen, K. K.: Early Holocene climate oscillations recorded in three Greenland ice cores, Quaternary Science Reviews, 26, 1907–1914, doi:10.1016/j.quascirev.2007.06.015.Abstract, 2007.

Rasmussen, S. O., Bigler, M., Blockley, S. P., Blunier, T., Buchardt, S. L., Clausen, H. B., Cvijanovic, I., Dahl-Jensen, D., Johnsen, S. J., Fischer, H., Gkinis, V., Guillevic, M., Hoek, W. Z., Lowe, J. J., Pedro, J. B., Popp, T., Seierstad, I. K., Steffensen, J. P., Svensson, A. M., Vallelonga, P., Vinther, B. M., Walker, M. J. C., Wheatley, J. J. and Winstrup, M.: A stratigraphic framework for abrupt climatic changes during the Last

Climate
of the Past

Discussions

Open Access

EGU

Glacial period based on three synchronized Greenland ice-core records: Refining and extending the
INTIMATE event stratigraphy, Quaternary Science Reviews, 106, 14–28,
doi:10.1016/j.quascirev.2014.09.007, 2014.

5   Reimer, P., Bard, E., Bayliss, A., Beck, J., Blackwell, P., Ramsey, C., Buck, C., Cheng, H., Edwards, R.,
Friedrich, M., Grootes, P., Guilderson, T., Haflidason, H., Hajdas, I., Hatté, C., Heaton, T., Hoffmann, D.,
Hogg, A., Hughen, K., Kaiser, K., Kromer, B., Manning, S., Niu, M., Reimer, R., Richards, D., Scott, E.,
Southon, J., Staff, R., Turney, C. and van der Plicht, J.: Intcal13 and Marine13 radiocarbon age calibration
curves 0–50,000 years cal BP, Radiocarbon, 55(4), 1869–1887, doi:10.2458/rc.v51i4.3569, 2013.

Renssen, H., Goosse, H. and Fichefet, T.: Simulation of Holocene cooling events in a coupled climate model,
10   Quaternary Science Reviews, 26(15–16), 2019–2029, doi:10.1016/j.quascirev.2007.07.011, 2007.

Rind, D.: The Sun's Role in Climate Variations, Science, 296(5568), 673–677, doi:10.1126/science.1069562,
2002.

Roden, J. S. and Ehleringer, J. R.: Observations of Hydrogen and Oxygen Isotopes in Leaf Water Confirm the
Craig-Gordon Model under Wide-Ranging Environmental Conditions, Plant Physiology, 120(August),
15   1165–1173, 1999.

Rozanski, K.: Deuterium and oxygen-18 in European Groundwaters - Links to Atmospheric Circulation in the
Past, Chemical Geology, 52, 349–363, 1985.

Rozanski, K., Araguás-Araguás, L. and Gonfiantini, R.: Isotopic patterns in modern global precipitation, Climate
change in continental isotopic records, 1–36, 1993.

20   Sachse, D., Radke, J. and Gleixner, G.: Hydrogen isotope ratios of recent lacustrine sedimentary n-alkanes
record modern climate variability, Geochimica et Cosmochimica Acta, 68(23), 4877–4889,
doi:http://dx.doi.org/10.1016/j.gca.2004.06.004, 2004.

Sachse, D., Billault, I., Bowen, G. J., Chikaraishi, Y., Dawson, T. E., Feakins, S. J., Freeman, K. H., Magill, C.
R., Mcinerney, F. A., van der Meer, M. T. J., Polissar, P., Robins, R. J., Sachs, J. P., Schmidt, H.-L.,
25   Sessions, A. L., White, J. W. C. and West, J. B.: Molecular Paleohydrology: Interpreting the Hydrogen-
Isotopic Composition of Lipid Biomarkers from Photosynthesizing Organisms, Annual Reviews, 40, 221–
249, doi:10.1146/annurev-earth-042711-105535, 2012.

Santrucek, J., Kveton, J., Setlik, J. and Bulickova, L.: Spatial Variation of Deuterium Enrichment in Bulk Water
of Snowgum Leaves, Plant Physiology, 143(1), 88–97, doi:10.1104/pp.106.089284, 2007.

30   Sauer, P. E., Eglinton, T. I., Hayes, J. M., Schimmelmann, A. and Sessions, A. L.: Compound-specific D/H
ratios of lipid biomarkers from sediments as a proxy for environmental and climatic conditions,
Geochimica et Cosmochimica Acta, 65(2), 213–222, doi:http://dx.doi.org/10.1016/S0016-7037(00)00520-
2, 2001.

Scharf, B. W. and Menn, U.: Hydrology and morphometry, in In Limnology of Eifel maar lakes, edited by B.
35   Scharf and S. Björk, pp. 43–62, E. Schweizerbart, Stuttgart, Germany., 1992.

Schmidt, H.-L., Werner, R. A. and Roßmann, A.: ^{18}O Pattern and biosynthesis of natural plant products,
Phytochemistry, 58(1), 9–32, doi:http://dx.doi.org/10.1016/S0031-9422(01)00017-6, 2001.

Sessions, A. L., Burgoyne, T. W., Schimmelmann, A. and Hayes, J. M.: Fractionation of hydrogen isotopes in
lipid biosynthesis, Organic Geochemistry, 30, 1193–1200, 1999.

40   Sirocko, F., Dietrich, S., Veres, D., Grootes, P. M., Schaber-mohr, K., Seelos, K., Nadeau, M., Kromer, B.,
Rothacker, L., Röhner, M., Krbetschek, M., Appleby, P., Hambach, U., Rolf, C., Sudo, M. and Grim, S.:
Multi-proxy dating of Holocene maar lakes and Pleistocene dry maar sediments in the Eifel , Germany,
Quaternary Science Reviews, 62, 56–76, doi:10.1016/j.quascirev.2012.09.011, 2013.

Sirocko, F., Knapp, H., Dreher, F., Förster, M. W., Albert, J., Brunck, H., Veres, D., Dietrich, S., Zech, M.,
45   Hambach, U., Röhner, M., Rudert, S., Schwibus, K., Adams, C. and Sigl, P.: The ELSA-Vegetation-Stack:
Reconstruction of Landscape Evolution Zones (LEZ) from laminated Eifel maar sediments of the last
60,000 years, Global and Planetary Change, 142, 108–135, doi:10.1016/j.gloplacha.2016.03.005, 2016.

Stenni, B., Masson-Delmotte, V., Selmo, E., Oerter, H., Meyer, H., Röthlisberger, R., Jouzel, J., Cattani, O.,
Falourd, S., Fischer, H., Hoffmann, G., Iacumin, P., Johnsen, S. J., Minster, B. and Udisti, R.: The
50   deuterium excess records of EPICA Dome C and Dronning Maud Land ice cores (East Antarctica),
Quaternary Science Reviews, 29, 146–159, doi:10.1016/j.quascirev.2009.10.009, 2010.

Sternberg, L. and Ellsworth, P. F. V.: Divergent Biochemical Fractionation, Not Convergent Temperature,
Explains Cellulose Oxygen Isotope Enrichment across Latitudes, PLoS ONE, 6(11), e28040,
doi:10.1371/journal.pone.0028040, 2011.

55   Sternberg, L. S. L.: D/H ratios of environmental water recored by D/H ratios of plants lipids, Nature, 336, 403–
405, doi:10.1038/332141a0, 1988.

Sternberg, L. S. L.: Comment on "Oxygen isotope ratios ($^{18}O/^{16}O$) of hemicellulose-derived sugar biomarkers in
plants, soils and sediments as paleoclimate proxy I: Insight from a climate chamber experiment" by Zech et
al. (2014), Geochimica et Cosmochimica Acta, 141, 677–679, doi:10.1016/j.gca.2014.04.051, 2014.

60   Sternberg, L. S. L., DeNiro, M. J. and Savidge, R. A.: Oxygen Isotope Exchange between Metabolites and Water
during Biochemical Reactions Leading to Cellulose Synthesis, Plant Physiology, 82, 423–427, 1986.

Stuiver, M. and Braziunas, T. F.: The Solar Component of the Atmospheric ^{14}C Record, in Secular Solar and

Geomagnetic Variations in the Last 10,000 Years, edited by F. R. Stephenson and A. W. Wolfendale, pp. 245–266, Springer, Dordrecht., 1988.

Stumpp, C., Klaus, J. and Stichler, W.: Analysis of long-term stable isotopic composition in German precipitation, Journal of Hydrology, 517, 351–361, doi:10.1016/j.jhydrol.2014.05.034, 2014.

5 Terwilliger, V. J., Kitajima, K., Le Roux-Swarthout, D. J., Mulkey, S. and Wright, S. J.: Intrinsic water-use efficiency and heterotrophic investment in tropical leaf growth of two Neotropical pioneer tree species as estimated from $\delta^{13}C$ values, New Phytologist, 152(2), 267–281, doi:10.1046/j.0028-646X.2001.00252.x, 2001.

Terwilliger, V. J., Betancourt, J. L., Leavitt, S. W. and Van De water, P. K.: Leaf cellulose δD and $\delta^{18}O$ trends
10 with elevation differ in direction among co-occurring, semiarid plant species, Geochimica et Cosmochimica Acta, 66(22), 3887–3900, doi:10.1016/S0016-7037(02)00964-X, 2002.

Thornalley, D. J. R., Elderfield, H. and McCave, I. N.: Holocene oscillations in temperature and salinity of the surface subpolar North Atlantic, Nature, 457(7230), 711–714, doi:10.1038/nature07717, 2009.

Thornalley, D. J. R., McCave, I. N. and Elderfield, H.: Freshwater input and abrupt deglacial climate change in
15 the North Atlantic, Paleoceanography, 25(1), 1–16, doi:10.1029/2009PA001772, 2010.

Thornalley, D. J. R., Elderfield, H. and McCave, I. N.: Reconstructing North Atlantic deglacial surface hydrography and its link to the Atlantic overturning circulation, Global and Planetary Change, 79(3–4), 163–175, doi:10.1016/j.gloplacha.2010.06.003, 2011.

Tipple, B. J., Berke, M. A., Doman, C. E., Khachaturyan, S. and Ehleringer, J. R.: Leaf-wax n-alkanes record the
20 plant-water environment at leaf flush, Proceedings of the National Academy of Sciences, 110(7), 2659–2664, doi:10.1073/pnas.1213875110, 2013.

Tipple, B. J., Berke, M. A., Hambach, B., Roden, J. S. and Ehleringer, J. R.: Predicting leaf wax n-alkane $^2H/^1H$ ratios: Controlled water source and humidity experiments with hydroponically grown trees confirm predictions of Craig-Gordon model, Plant, Cell and Environment, 38(6), 1035–1047,
25 doi:10.1111/pce.12457, 2015.

Tuthorn, M., Zech, M., Ruppenthal, M., Oelmann, Y., Kahmen, A., del Valle, H. F., Wilcke, W. and Glaser, B.: Oxygen isotope ratios ($^{18}O/^{16}O$) of hemicellulose-derived sugar biomarkers in plants, soils and sediments as paleoclimate proxy II: Insight from a climate transect study, Geochimica et Cosmochimica Acta, 126, 624–634, doi:http://dx.doi.org/10.1016/j.gca.2013.11.002, 2014.

30 Tuthorn, M., Zech, R., Ruppenthal, M., Oelmann, Y., Kahmen, A., del Valle, H. F., Eglinton, T., Rozanski, K. and Zech, M.: Coupling δ^2H and $\delta^{18}O$ biomarker results yields information on relative humidity and isotopic composition of precipitation - a climate transect validation study, Biogeosciences, 12, 3913–3924, doi:10.5194/bg-12-3913-2015, 2015.

Voelker, S. L., Brooks, J. R., Meinzer, F. C., Roden, J., Pazdur, A., Pawelczyk, S., Hartsough, P., Snyder, K.,
35 Plavcova, L. and Santrucek, J.: Reconstructing relative humidity from plant $\delta^{18}O$ and δD as deuterium deviations from the global meteoric water line, Ecological Applications, 24(5), 960–975, doi:10.1890/13-0988.1, 2014.

Voelker, S. L., Stambaugh, M. C., Guyette, R. P., Feng, X., Grimley, D. A., Leavitt, S. W., Panyushkina, I., Grimm, E. C., Marsicek, J. P., Shuman, B. and Brandon Curry, B.: Deglacial hydroclimate of
40 midcontinental North America, Quaternary Research (United States), 83(2), 336–344, doi:10.1016/j.yqres.2015.01.001, 2015.

Volkman, J. K., Barrett, S. M., Blackburn, S. I., Mansour, M. P., Sikes, E. L. and Gelin, F.: Microalgal biomarkers: A review of recent research developments, Organic Geochemistry, 29(5--7), 1163–1179, doi:http://dx.doi.org/10.1016/S0146-6380(98)00062-X, 1998.

45 Vonmoos, M., Beer, J. and Muscheler, R.: Large variations in Holocene solar activity: Constraints from ^{10}Be in the Greenland Ice Core Project ice core, Journal of Geophysical Research: Space Physics, 111(10), 1–14, doi:10.1029/2005JA011500, 2006.

Wagner, F., Bohncke, S. J. P., Dilcher, D. L., Kürschner, W. M., van Geel, B. and Visscher, H.: Century-Scale Shifts in Early Holocene Atmospheric CO_2 Concentration, Science, 284(June), 1971–1974, 1999.

50 Walker, C. D. and Brunel, J.-P.: Examining Evapotranspiration in a Semi-Arid Region using Stable Isotopes of Hydrogen and Oxygen, Journal of Hydrology, 118, 55–75, 1990.

Walker, M., Johnsen, S., Rasmussen, S. O., Popp, T., Steffensen, J.-P., Gibbard, P., Hoek, W., Lowe, J., Andrews, J., Björck, S., Cwynar, L. C., Hughen, K., Kershaw, P., Kromer, B., Litt, T., Lowe, D. J., Nakagawa, T., Newnham, R. and Schwander, J.: Formal definition and dating of the GSSP (Global
55 Stratotype Section and Point) for the base of the Holocene using the Greenland NGRIP ice core, and selected auxiliary records, Journal of Quaternary Science, 24(1), 3–17, doi:10.1002/jqs, 2009.

Walthert, L., Graf, U., Kammer, A., Luster, J., Pezzotta, D., Zimmermann, S. and Hagedorn, F.: Determination of organic and inorganic carbon, $\delta^{13}C$, and nitrogen in soils containing carbonates after acid fumigation with HCl, Journal of Plant Nutrition and Soil Science, 173(2), 207–216, doi:10.1002/jpln.200900158, 2010.

60 Wang, X.-F., Yakir, D. and Avisha, M.: Non-climatic variations in the oxygen isotopic composition of plants, Global Change Biology, 4, 835–849, 1998.

Waterhouse, J. S., Cheng, S., Juchelka, D., Loader, N. J., McCarroll, D., Switsur, V. R. and Gautam, L.:

Position-specific measurement of oxygen isotope ratios in cellulose: Isotopic exchange during heterotrophic cellulose synthesis, Geochimica et Cosmochimica Acta, 112(0), 178–191, doi:http://dx.doi.org/10.1016/j.gca.2013.02.021, 2013.

Weninger, B. and Jöris, O.: A ^{14}C age calibration curve for the last 60 ka: the Greenland-Hulu U/Th timescale and its impact on understanding the Middle to Upper Paleolithic transition in Western Eurasia, Journal of Human Evolution, 55(5), 772–781, doi:https://doi.org/10.1016/j.jhevol.2008.08.017, 2008.

Wolfe, B. B., Edwards, T. W. D. and Aravena, R.: Changes in carbon and nitrogen cycling during tree-line retreat recorded in the isotopic content of lacustrine organic matter, western Taimyr Peninsula, Russia, Holocene, 9(2), 215–222, doi:10.1191/095968399669823431, 1999.

Wolfe, B. B., Aravena, R., Abbott, M. B., Seltzer, G. O. and Gibson, J. J.: Reconstruction of paleohydrology and paleohumidity from oxygen isotope records in the Bolivian Andes, Palaeogeography, Palaeoclimatology, Palaeoecology, 176(1–4), 177–192, doi:http://dx.doi.org/10.1016/S0031-0182(01)00337-6, 2001.

Yakir, D. and DeNiro, M. J.: Oxygen and Hydrogen Isotope Fractionation during Cellulose Metabolism in *Lemna gibba* L., Plant Ecology, 93, 325–332, 1990.

Zech, M. and Glaser, B.: Compound-specific $\delta^{18}O$ analyses of neutral sugars in soils using gas chromatography-pyrolysis-isotope ratio mass spectrometry: problems, possible solutions and a first application, Rapid Communications in Mass Spectrometry, 23, 3522–3532, doi:10.1002/rcm, 2009.

Zech, M., Zech, R. and Glaser, B.: A 240,000-year stable carbon and nitrogen isotope record from a loess-like palaeosol sequence in the Tumara Valley, Northeast Siberia, Chemical Geology, 242, 307–318, doi:10.1016/j.chemgeo.2007.04.002, 2007.

Zech, M., Zech, R., Buggle, B. and Zöller, L.: Novel methodological approaches in loess research – interrogating biomarkers and compound-specific stable isotopes, Eiszeitalter und Gegenwart – Quaternary Science Journal, 60(1), 170–187, doi:10.3285/eg.60.1.12, 2011.

Zech, M., Werner, R. A., Juchelka, D., Kalbitz, K., Buggle, B. and Glaser, B.: Absence of oxygen isotope fractionation/exchange of (hemi-) cellulose derived sugars during litter decomposition, Organic Geochemistry, 42(12), 1470–1475, doi:http://dx.doi.org/10.1016/j.orggeochem.2011.06.006, 2012.

Zech, M., Tuthorn, M., Detsch, F., Rozanski, K., Zech, R., Zöller, L., Zech, W. and Glaser, B.: A 220 ka terrestrial $\delta^{18}O$ and deuterium excess biomarker record from an eolian permafrost paleosol sequence, NE-Siberia, Chemical Geology, 360–361, 220–230, doi:http://dx.doi.org/10.1016/j.chemgeo.2013.10.023, 2013a.

Zech, M., Tuthorn, M., Glaser, B., Amelung, W., Huwe, B., Zech, W., Zöller, L. and Löffler, J.: Natural abundance of $\delta^{18}O$ of sugar biomarkers in topsoils along a climate transect over the Central Scandinavian Mountains, Norway, Journal of Plant Nutrition and Soil Science, 176(1), 12–15, doi:10.1002/jpln.201200365, 2013b.

Zech, M., Tuthorn, M., Schlütz, F., Zech, W. and Glaser, B.: A 16-ka $\delta^{18}O$ record of lacustrine sugar biomarkers from the High Himalaya reflects Indian Summer Monsoon variability, Journal of Paleolimnology, 51, 241–251, doi:10.1007/s10933-013-9744-4, 2014a.

Zech, M., Mayr, C., Tuthorn, M., Leiber-Sauheitl, K. and Glaser, B.: Oxygen isotope ratios ($^{18}O/^{16}O$) of hemicellulose-derived sugar biomarkers in plants, soils and sediments as paleoclimate proxy I: Insight from a climate chamber experiment, Geochimica et Cosmochimica Acta, 126(0), 614–623, doi:http://dx.doi.org/10.1016/j.gca.2013.10.048, 2014b.

Zech, M., Mayr, C., Tuthorn, M., Leiber-Sauheitl, K. and Glaser, B.: Reply to the comment of Sternberg on "Zech et al. (2014) Oxygen isotope ratios ($^{18}O/^{16}O$) of hemicellulose-derived sugar biomarkers in plants, soils and sediments as paleoclimate proxy I: Insight from a climate chamber experiment. GCA, Geochimica et Cosmochimica Acta, 141(0), 680–682, doi:10.1016/j.gca.2014.04.051, 2014c.

Zolitschka, B.: A 14,000 year sediment yield record from western Germany based on annually laminated lake sediments, Geomorphology, 22(1), 1–17, doi:10.1016/S0169-555X(97)00051-2, 1998.
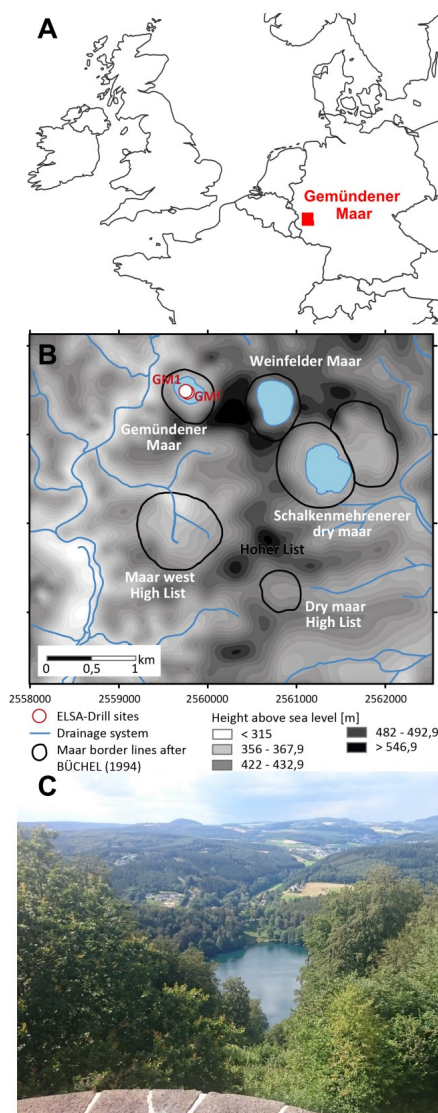
Figures

Fig. 1: (A) Location of the Lake Gemündener Maar in the Eifel Region in Germany (generated using OpenStreetMap homepage, www.openstreetmap.org). (B) Digital terrain model and
5   drainage system of the closer surrounding of Lake Gemündener Maar with maar borders according to Büchel (1994), representing the size of the crater. In addition, the core position is displayed (GM1; 50°10'39.853"N, 6°50'12.912"E) along with the short core GMf (not part of the study) marked as ELSA-Drill sites. Both cores are part of the Eifel Laminated Sediment Archive Project (ELSA-Project). (C) Photo of Lake Gemündener Maar showing the steep and
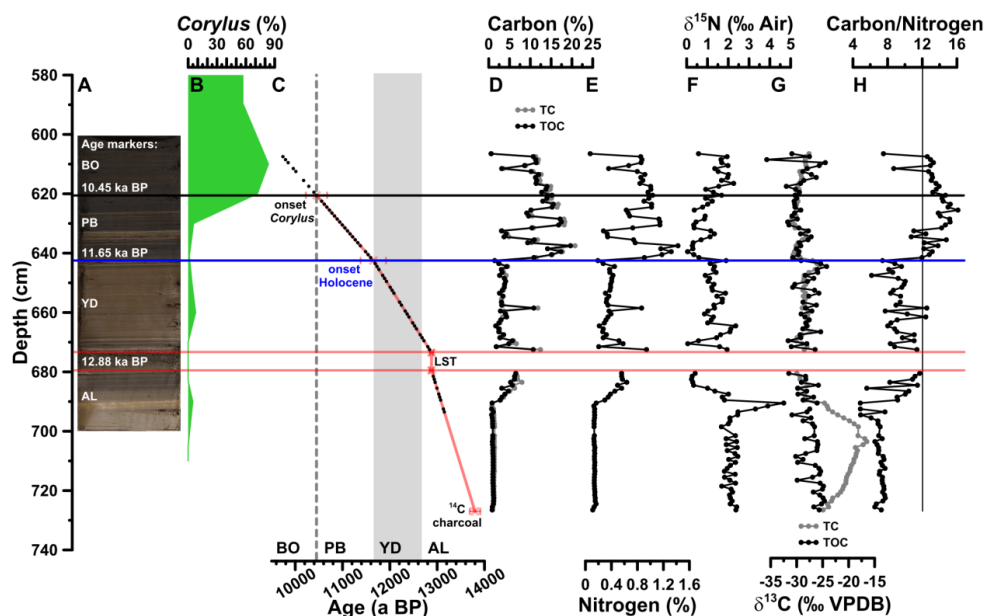10   densely vegetated catchment (from M. Zech).

Fig. 2: (A) Photo of the investigated GM1 core section, with regard to the biomarkers (607 to 694 cm depth), including age markers. (B) Depth profile of *Corylus* pollen (derived from unpublished pollen analysis by F. Sirocko). (C) Age-depth model of the full investigated GM1 section (606 to 727 cm depth) consisting of a ^{14}C dated piece of charcoal, the Laacher See Tephra (LST), the onset of the Holocene (blue line) and *Corylus* pollen (black line). Additionally, the biomarker sampling points (black points) are displayed. Depth profiles of (D) total and total organic carbon (TC, TOC), (E) total nitrogen (TN), (F) bulk stable nitrogen isotope composition (δ^{15}N), (G) TC and TOC stable carbon isotope composition (δ^{13}C$_{TC}$, δ^{13}C$_{TOC}$), (H) Carbon to nitrogen ratio based on total organic carbon and total nitrogen (TOC/TN). The vertical line in (H) indicates a C/N ratio threshold of 12. AL = Allerød, YD = Younger Dryas, PB = Preboreal, and BO = Boreal.
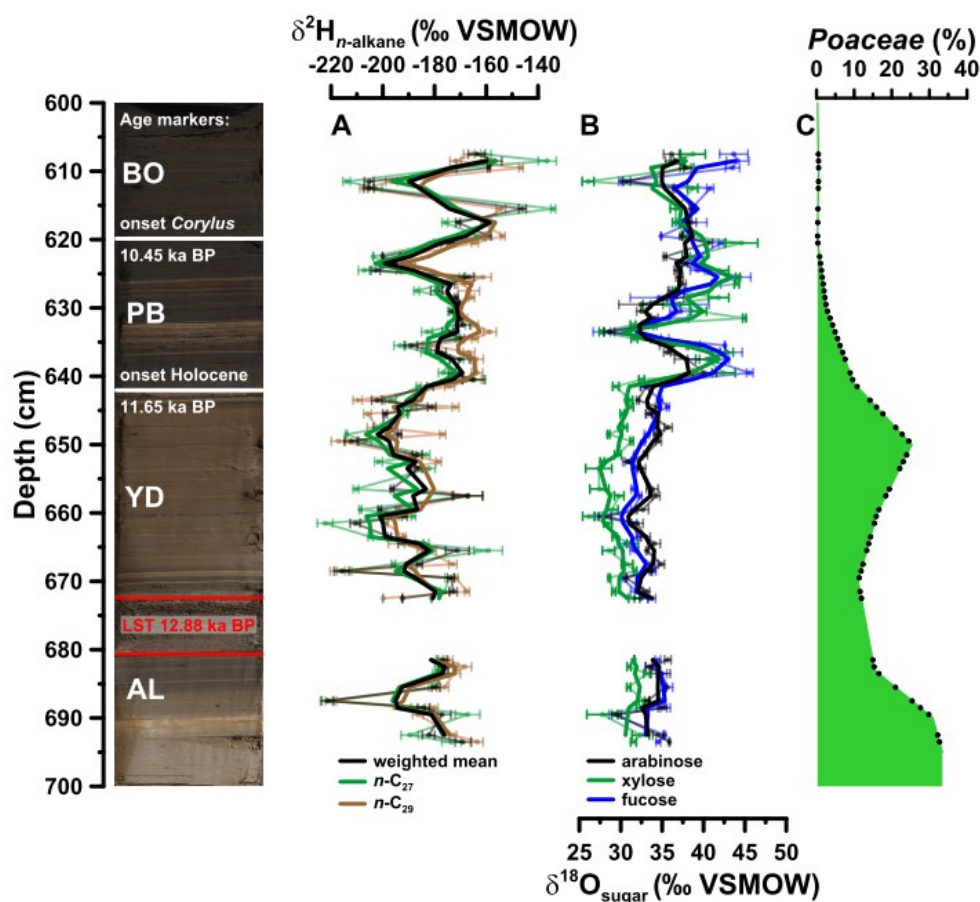
Climate
of the Past
Open Access
Discussions
EGU

Fig. 3: (A) Depth profiles of compound-specific stable hydrogen isotope composition of the
individual alkanes n-C$_{27}$ and n-C$_{29}$ and the weighted mean (δ^2H$_{n\text{-alkane}}$). (B) Compound-specific
stable oxygen composition of the individual sugars arabinose, xylose and fucose (δ^{18}O$_{sugar}$). All

5   plots are shown with error bars representing standard measurement errors overlain by three
point moving averages (bold lines). (C) Depth profile of *Poaceae* pollen (derived from
unpublished pollen analysis by F. Sirocko). Additionally, the resampled data points (black
points) used for the grass correction procedures (Eq. 12 and 13) are displayed. In addition, the
GM1 core picture with the used age markers is displayed. AL = Allerød, LST = Laacher See

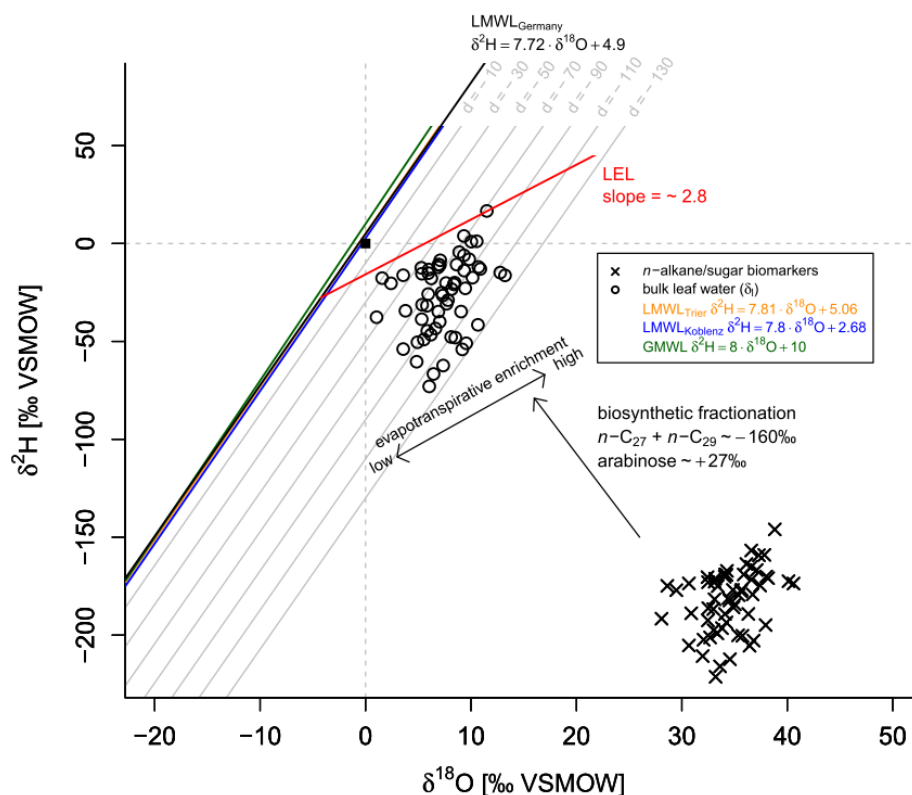10   Tephra, YD = Younger Dryas, PB = Preboreal, and BO = Boreal.

Fig. 4: (A) Conceptual framework of the applied $\delta^2H_{n\text{-alkane}}$-$\delta^{18}O_{sugar}$ approach displayed as $\delta^{18}O$-δ^2H diagram showing the measured n-alkanes (weighted mean of n-C_{27} and n-C_{29}) and sugar (arabinose) biomarkers (black crosses), the reconstructed leaf water (δ_l; open circles), the

5   global meteoric water line (GMWL, green line) and the local meteoric water lines of Germany (LWML$_{Germany}$, black line), Trier (LWML$_{Trier}$, yellow line) and Koblenz (LWML$_{Koblenz}$, blue line). The arrows indicate natural processes of evaportranspirative enrichment of leaf water and biosynthetic fractionation during biomarker synthesis. Grey lines indicate the parallel distance between the individual reconstructed evaporative site leaf water points and the LMWL$_{Germany}$,

10   expressed as d = δ^2H – 7.72 · $\delta^{18}O$, which can serve as proxy for mean daytime vegetation period relative humidity.
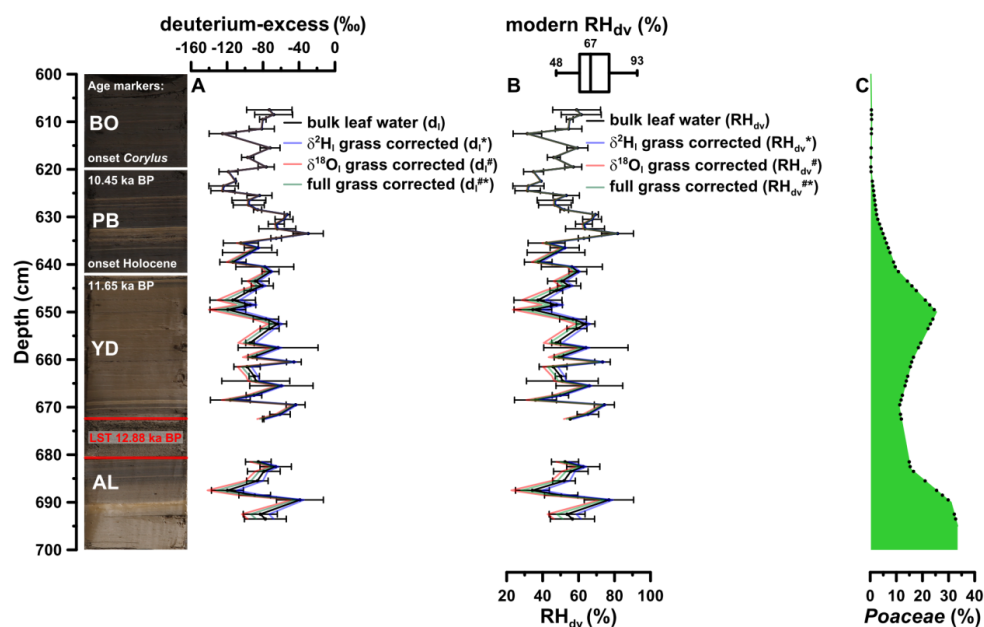
Fig. 5: (A) Reconstructed deuterium-excess depth profiles using leaf water (d_l; black line) in comparison to solely *n*-alkane grass corrected d_l* values (light blue line), solely arabinose grass corrected $d_l^{\#}$ values (light red line), and full grass corrected $d_l^{\#}$* values (light green line). The error bar of d_l value are calculated according to Eq. (7). (B) The corresponding RH_{dv} records to (A). Modern relative air humidity variability during daytime and vegetation period is displayed as boxplot derived from the adjacent meteorological station Nürburg-Barweiler, using monthly means from April to October between 6 a.m. and 7 p.m. (based on hourly data from 1995 to 2015; Deutscher Wetterdienst, 2016). The bold numbers within the boxplot represents the maximum, median, and minimum value, respectively. (C) Depth profile of *Poaceae* pollen (derived from unpublished pollen analysis by F. Sirocko). Additionally, the resampled data points (black points) are displayed. The GM1 core picture with the used age markers are displayed on the left. AL = Allerød, LST = Laacher See Tephra, YD = Younger Dryas, PB = Preboreal, and BO = Boreal.
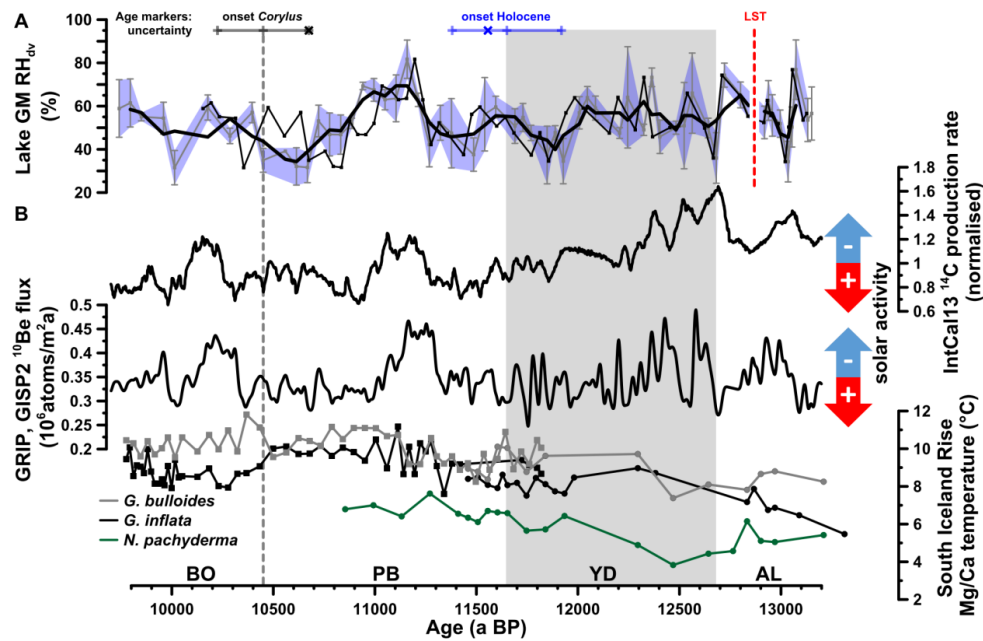
Fig. 6: (A) Reconstructed Lake Gemündener Maar (GM) RH_{dv} values, overlain by a three point moving averages (thick black line). Error bars and the blue shaded area indicate uncertainties introduced by $^2H_{n\text{-alkane}}$/$^{18}O_{arabinose}$ measurements calculated according to error propagation (Eq.

5   7). In addition, the derived 68% uncertainty of the onset of *Corylus* pollen (black) and the Holocene (blue) are shown. The crosses within these lines represents the adjusted ages according to the Monte-Carlo-Simulation based correlation procedure to the IntCal13 ^{14}C production rate. The GM RH_{dv} values are additionally shown on an optimized age-depth scale (thin black line with squares). Please note that the ^{14}C charcoal age is also covered by an error

10   and was as well included in the adjustment procedure but not shown in this graph for clarity reasons. (B) IntCal13 ^{14}C production rate, Greenland ice-core (GRIP, GISP2) ^{10}Be flux record (both from Muscheler et al., 2014) and South Iceland Rise planktic Mg/Ca derived water temperatures from RAPiD-12-1K (squares; 9,800 to 11,800 a BP) and RAPiD-15-4P (circles; 10,900 to 13,100 a BP). RAPiD-12-1K and RAPiD-15-4P *G. bulloides* and *G. inflat* data from

15   Thornalley et al. (2009) and Thornalley et al. (2010), respectively. RAPiD-15-4P *N. pachyderma* data from Thornalley et al. (2011). Note that each record is plotted on its own timescale (planktonic Mg/Ca data see (Thornalley et al., 2009, 2010), ^{10}Be data on GICC05 (Rasmussen et al., 2006), ^{14}C data on IntCal13 calibration curve (Reimer et al., 2013) and RH_{dv} data on Lake GM age-depth model, see Fig. 2C). AL = Allerød, LST = Laacher See Tephra,

20   YD = Younger Dryas, PB = Preboreal, and BO = Boreal.

Climate
of the Past
Discussions

Table

Tab. 1: Scenarios (1-4) comprising the different reconstructed leaf water parameters based on the n-alkane/sugar biomarker, the respective equations used for this reconstruction, the resulting deuterium-excess of leaf water based on the reconstructed leaf water as input for Eq. (5) and

5   the finally derived relative air humidity values during daytime and vegetation period (RH_{dv}) with this equation.

scenario	leaf water reconstructed from n-alkane/sugar biomarkers	equations used for leaf water reconstruction	resulting deuterium-excess of leaf water as input for Eq. (5)	relative air humidity during daytime and vegetation period according Eq. (5)
1	$\delta^2H_l/\delta^{18}O_l$	(8) and (9)	d_l	RH_{dv}
2	$\delta^2H_l{}^*/\delta^{18}O_l$	(8) and (9) + (11)	$d_l{}^*$	$RH_{dv}{}^*$
3	$\delta^2H_l/\delta^{18}O_l{}^\#$	(8) + (10) and (9)	$d_l{}^\#$	$RH_{dv}{}^\#$
4	$\delta^2H_l{}^*/\delta^{18}O_l{}^\#$	(8) + (10) and (9) + (11)	$d_l{}^*{}^\#$	$RH_{dv}{}^*{}^\#$